Notch signaling via Hey1 and Id2b regulates Müller glia's regenerative response to retinal injury

Aresh Sahu, Sulochana Devi, Jonathan Jui and Daniel Goldman*

Michigan Neuroscience Institute and Department of Biological Chemistry

University of Michigan, Ann Arbor, MI 48109

*Correspondence: Daniel Goldman, neuroman@umich.edu

Key words: stem cell, Müller glia, retina, regeneration, Notch, Ascl1, hey1, dll4, notch3, reprogramming

Abstract

Unlike mammals, zebrafish can regenerate a damaged retina. Key to this regenerative response are Müller glia (MG) that divide and produce progenitors for retinal repair. Although factors regulating MG's decision to divide remain mostly unknown, a certain threshold of neuron death must be exceeded in order for MG to engage in a regenerative response. A role for Notch signaling in this process is indicated since its inhibition expands the zone of injury-responsive MG following a focal injury. Our data show that injury-dependent changes in Dll4 and Dlb control Notch signaling in MG and that Hey1 and Id2b are downstream effectors that regulate proliferation of MG and MG-derived progenitors. Although we find Hey1 and Id2b can inhibit proliferation of MG-derived progenitors, only Hey1 is able to regulate MG's injury response threshold. Remarkably, Hey1 suppression is sufficient to recapitulate the effects of Notch inhibition on MG's injury response threshold.

Introduction

Although the mammalian and zebrafish retina share structure and function, only zebrafish are able to regenerate a damaged retina. Key to this regenerative response are Müller glia (MG) that normally help maintain retinal structure and homeostasis(Goldman 2014, Lahne et al 2020, Lenkowski & Raymond 2014, MacDonald et al 2015, Reichenbach & Bringmann 2013, Wan & Goldman 2016). MG are the only retinal cells that exhibit a radial glial morphology with processes extending longitudinally and laterally that allow MG to interact with and sample their environment.

A focal injury to the zebrafish retina stimulates MG, immediately flanking the injury site, to mount a regenerative response(Goldman 2014, Lahne et al 2020, Lenkowski & Raymond 2014, Wan & Goldman 2016). This response includes changes in MG gene expression, signal transduction, and a self-renewing asymmetric cell division that produces a transient amplifying progenitor for retinal repair(Hoang et al 2020, Lee et al 2020, Nagashima et al 2013, Powell et al 2013, Ramachandran et al 2010a, Ramachandran et al 2011, Ramachandran et al 2012, Sifuentes et al 2016, Wan & Goldman 2017, Wan et al 2012, Wan et al 2014, Zhao et al 2014b). Although these regenerative events are not engaged by MG in the injured mammalian retina, both zebrafish and mammalian MG initiate a gliotic response to injury that is characterized by hypertrophy and increased expression of intermediate filament proteins(Hoang et al 2020, Thomas et al 2016).

It remains unknown why mammalian MG cannot mount a regenerative response like their zebrafish counterparts. However, their basal state likely dictates their regenerative/stem cell potential. Recent studies comparing MG transcriptomes across species, as well as targeted perturbation of specific genes and signaling pathways, have identified differences between fish and mammalian MG gene expression programs(Elsaeidi et al 2018, Hoang et al 2020, Lee et al 2020, Sifuentes et al 2016). For example, Tgfb3 and Notch signaling pathways are active in adult zebrafish MG(Elsaeidi et al 2018, Lee et al 2020, Wan & Goldman 2017, Wan et al 2012), but not in those from adult mice(Lee et al 2020, Nelson et al 2011). Interestingly, Tgfb3 stimulates Notch signaling in the zebrafish retina(Lee et al 2020), and Notch signaling helps maintain radial glial stem cells in a quiescent state in the zebrafish and mouse brain(Alunni et al 2013, Engler et al 2018, Kawai et al 2017, Than-Trong et al 2018).

Like that observed for radial glial stem cells, Notch signaling must be suppressed for MG proliferation and retina regeneration (Campbell et al 2021, Conner et al 2014, Elsaeidi et al 2018, Wan & Goldman 2017, Wan et al 2012). Furthermore, pan-retinal Notch inhibition increases the number of MG that engage in a regenerative response in light and needle poke injury models(Campbell et al 2021, Wan & Goldman 2017, Wan et al 2012), and Notch inhibition enhances spontaneous MG proliferation in uninjured retinas treated with growth factors, cytokines, or forced expression of Ascl1a and Lin28a(Conner et al 2014, Elsaeidi et al 2018, Wan & Goldman 2017).

Using a needle poke injury model we have shown that MG at the injury site, and immediately flanking it, engage in a regenerative response that is characterized by their cell division(Fausett & Goldman 2006). This restricted MG response suggests injury signals do not travel far from the injury site. However, we have shown that this localized injury response can be expanded by combining needle poke injury with pan-retinal Notch inhibition(Wan & Goldman 2017, Wan et al 2012). This result is consistent with the idea that Notch signaling regulates MG's injury response threshold. In this scenario, MG only enter a proliferative state when exposed to injury-related signals that exceed a certain threshold that is sufficient to suppress basal Notch signaling in MG.

Because Notch signaling controls MG's responsiveness to injury-derived signals, understanding its mechanism of action may not only inform us of the underlying mechanism, but also may suggest strategies for enhancing MG's regenerative potential in mammals. One recent study investigating Notch ligand and receptor encoding genes concluded Dlb, acting via the Notch3 receptor, maintains MG quiescence and suppresses MG proliferation in the light damaged retina(Campbell et al 2021). However, the mechanism by which these factors act to regulate MG's injury response remains unknown.

To this end we investigated how Notch signaling is controlled in quiescent MG residing in the uninjured retina and identified its downstream target genes. We report that Notch signaling in MG is largely controlled by *dll4*, *dlb*, and *notch3* gene expression. Suppression or inactivation of any of these Notch signaling components lowers MG's injury response threshold and enhances proliferation of MG-derived progenitors. Interestingly, we found that Notch signaling regulates MG's injury response threshold through altering chromatin accessibility of a subset of regeneration-associated genes and by engaging certain regeneration-associated gene expression programs. Importantly, we identified two Notch target genes, *hey1* and *id2b*, that mediate the effects of Notch signaling on retina regeneration. Our studies indicate that Hey1 regulates MG's injury response threshold, while both Hey1 and Id2b regulate proliferation of MG-derived progenitors.

Results

Injury-dependent regulation of MG gene expression and chromatin accessibility

Previous studies suggested that Notch signaling promotes MG differentiation and stimulates MG-specific gene expression(Bernardos et al 2005, Jadhav et al 2006, Nelson et al 2011, Scheer et al 2001). Therefore, we wondered if injury-dependent suppression of Notch signaling resulted in a loss of MG identity that may be reflected in reduced expression of MG-specific genes. To investigate this, we compared previously generated RNAseq data sets prepared from MG in the uninjured retina of *gfap:GFP* fish with those from activated MG and MG-derived progenitors isolated at 2 days post needle poke injury (dpi) from *1016 tuba1a:GFP* fish(Lee et al 2020). At this time point, most MG are in an activated state with some beginning to proliferate(Fausett & Goldman 2006). This analysis identified 4,425 differentially expressed genes with 2,579 showing increased expression (fold change $\geq \pm$ 1.5; Figure 1a). We validated a few of these genes (Figure 1b; Figure 1-figure supplement 1a). Some of these regulated genes, like *ascl1a* and *hbegfa,* have already been shown to play important roles during retina regeneration(Fausett et al 2008, Gorsuch et al 2017, Ramachandran et al 2010a, Ramachandran et al 2011, Wan et al 2012). Interestingly, genes associated with MG identity, like *glula* and *rlbp1a* were repressed, while other MG genes, like *gfap*, *sox2*, *apoeb*, and *fabp7a* were induced (Figure 1-figure supplement 1b). These data suggested that suppression of MG identity genes may not be as critical as the instatement of regeneration-associated gene expression programs in determining MG's regenerative capacity.

We next investigated if changes in chromatin accessibility correlated with the transition of MG from a quiescent to an activated state. For this analysis, ATACseq was used to probe chromatin accessibility in nuclei from quiescent MG isolated from uninjured *gfap:GFP* fish and nuclei from activated MG isolated from injured (needle poke, 2 dpi) *1016 tuba1a:GFP* fish(Buenrostro et al 2015). We mapped injury-dependent differential chromatin accessibility to 5,684 genes (Figure 1c). On a global scale, ATACseq revealed a slight bias towards open chromatin in activated MG with 15,595 regions exhibiting an increase and 13,049 regions exhibiting a decrease in chromatin accessibility. However, when these regions were annotated to different genic features and compared to all annotated regions, increased chromatin accessibility was enriched in intergenic regions, while decreased chromatin accessibility was enriched in the 5' UTR, promoters, and 1-5 kb region upstream of the transcription start site (Figure 1-figure supplement 1c).

To correlate injury-dependent changes in gene expression with changes in chromatin accessibility, we intersected our RNAseq and ATACseq injury-regulated gene lists (Figure 1-table supplement 1). This analysis identified 1,311 injury-responsive MG genes with changes in chromatin accessibility (Fig. 1d; Figure1-figure supplement 1d). ~60% of the injury-induced genes and ~64% of the injury-repressed genes showed a corresponding change in chromatin accessibility (Figure 1d; Figure 1-table supplement 1). Importantly, many of these changes in chromatin accessibility included promoters and upstream sequences (Figure 1-figure supplement 1d; Figure 1-table supplement 2).

DAPT-dependent regulation of MG gene expression and chromatin accessibility

Notch repression with DAPT allows normally quiescent MG adjacent to the injury affected zone to mount a regenerative response(Wan & Goldman 2017, Wan et al 2012). To help understand how Notch inhibition accomplishes this, we used RNAseq to characterize the DAPT-regulated transcriptome in quiescent MG. For this analysis, uninjured *gfap:GFP* fish were treated +/-DAPT for 24 hours and GFP+ MG were purified by FACS. RNAseq identified 1,261 differentially expressed genes, with only 375 showing reduced expression following Notch inhibition (fold change $\geq \pm$ 1.5; Figure 2a). Interestingly, of these DAPT-regulated genes, 245 are also regulated by retinal injury and include regeneration-associated genes, like *ascl1a* and *hbegfa* (Figure 2a and b; Figure 2-figure supplement 2a and b; Figure 2-table supplement 3). Furthermore, although Notch signaling is necessary for MG differentiation during development(Bernardos et al 2005), genes conferring glial identity were generally unaffected by Notch signaling inhibition in adult fish (Figure 2-figure supplement 2c).

We next investigated the consequence of Notch signaling inhibition on MG chromatin accessibility. For this analysis, nuclei were isolated from GFP+ MG purified from uninjured *gfap:GFP* fish treated +/-DAPT and ATACseq was used to assay chromatin accessibility as previously described(Buenrostro et al 2015). On a global scale, inhibition of Notch signaling affected chromatin accessibility in a similar fashion as retinal injury with 16,990 regions showing increased and 12,413 regions showing decreased chromatin accessibility (Figure 2c). However, unlike that found with retinal injury, DAPT-treatment resulted in increased chromatin accessibility in 5' regions of genes including 5'UTR, promoters, and 1-5kb upstream regions, while intergenic regions appear to be enriched for closed chromatin (Figure 2-figure supplement 2d and e).

We mapped DAPT-dependent differential chromatin accessibility to 7,643 genes (Figure 2d), which exceeds those whose chromatin accessibility is regulated by retinal injury (Figure 1d). Interestingly, when examining promoter regions (1kb upstream of transcription start site) for differential chromatin accessibility, we found 156 promoters with reduced chromatin accessibility, and 3,871 promoters with increased chromatin accessibility (Figure 2-table supplement 4). This bias towards open chromatin was also observed in the 1-5kb region upstream of transcription start sites, where we observed 196 genes with reduced chromatin accessibility and 1,041 genes with increased chromatin accessibility (Figure 2-table supplement 4).

Of the genes whose chromatin accessibility changed with DAPT-treatment, 1,497 were also regulated by retinal injury (Figure 2d), which is similar to the number of genes showing changes in chromatin accessibility after retinal injury (Figure 1d). However, when we correlate injury-dependent gene regulation with changes in chromatin accessibility upstream of transcription start sites, we found a larger proportion of the injury-responsive genomic regions with increased chromatin accessibility following DAPT-treatment compared to retinal injury (1,175 vs 642) (Figures 1d and 2d; Figures 1 and 2-table supplements 2 and 4). Furthermore, ~67% of these latter increases in chromatin accessibility are associated with genes whose expression is increased in the injured retina.

Together, the above data suggests Notch inhibition in the uninjured retina lowers MG's injury response threshold by increasing chromatin accessibility and regulating the expression of certain key regeneration-associated genes.

Notch-dependent regulation of genes impacting MG reprogramming

We hypothesized that MG regeneration-associated genes that are also regulated in a similar direction by Notch signaling in the uninjured retina would identify a relatively small set of genes that may regulate MG's injury response threshold. Intersection of injury and Notch-regulated RNAseq data sets revealed 190 induced (basal value ≥5; fold change ≥1.5) and 55 repressed (basal value ≥50; fold change ≥1.5) genes (Figure 2b; Figure 2-figure supplement 2a and b; Figure 2-table supplement 5). The top 20 injury-responsive genes that were regulated in similar direction following DAPT-treatment are listed in Figure 2-figure supplement 2a.

DAPT is a γ-secretase inhibitor that can target over 100 substrates, of which Notch is only one(Xia 2019). To help narrow-in on Notch-regulated genes, we took advantage of *hsp70:DN-MAML* transgenic fish(Zhao et al 2014a). DN-MAML retains NICD-Rbpj binding activity, but lacks MAML's transcriptional activation domain and thus suppresses endogenous Notch-dependent gene activation(Maillard et al 2006, Maillard et al 2004). To identify MG genes regulated by DN-MAML in uninjured retina, we treated *gfap:mCherry* and *gfap:mCherry;hsp70:DN-MAML* fish with heat shock every 6 hours for 1 day and then FACS purified GFP+ MG for RNAseq. This analysis identified 1,122 differentially expressed genes with only 244 showing reduced expression (fold change ≥ ± 1.5; Figure 2-figure supplement 2f).

We next determined the intersection of injury-responsive MG genes that were also regulated in the same direction by DAPT and DN-MAML in the uninjured retina. Remarkably, this analysis identified 84 induced genes and 5 repressed genes (fold change ≥ ± 1.5) (Figure 2-table supplement 5 and genes marked with asterisk in Figure 2-figure supplement 2a). Thus, out of a total of 4,425 regeneration-associated genes, we have narrowed-in on 89 that are Notch-responsive in the uninjured retina and perhaps regulating MG's threshold response to retinal injury.

Notch-Hey1 signaling controls MG's injury response threshold

We were struck by the observation that *hey1* and *id2b* were the only transcriptional regulators consistently repressed in both the injured and Notch inhibited retina. Since Notch activation normally stimulates gene expression, *id2b* and *hey1* are good candidates for being direct Notch target genes. Inspection of the 3kb region upstream of their transcriptional start sites, revealed consensus Rbpj binding elements in the *hey1* gene (Figure 3a). Two of these elements are highly conserved in sequence and position when compared with orthologous genes from mouse and human (Figure 3a). To investigate if these putative Rbpj binding elements conferred Notch dependent regulation on *hey1* promoter activity we generated a *3kb-hey1:luciferase* vector with and without mutations in these 2

conserved Rbpj binding sites (Figure 3a). Transfection of HEK293 cells revealed increased *hey1* promoter activity in those cells co-transfected with *CMV:NICD*, and that this increased expression was abrogated by mutation of either Rbpj binding site (Figure 3b).

We next investigated if Hey1 and/or Id2b contributed to MG's injury response threshold. For this analysis, we knocked down their expression with either a splice blocking *hey1*-MO or a translation blocking *id2b*-MO (Figure 3-figure supplement 3a-c). MO effectiveness was determined in embryos, where injection of the *hey1*-MO resulted in *hey1* RNA intron-retention and injection of the *id2b*-MO with an *id2b*-GFP chimeric RNA resulted in reduced GFP expression (Figure 3-figure supplement 3b and c). Remarkably, only Hey1 knockdown increased MG proliferation and expanded the zone of injury-responsive MG (Figure 3c-e; Figure 3-figure supplement 3d). We confirmed this result using a CRISPR-based gene editing strategy where embryos were injected with *in vitro* transcribed *Cas9-nanos* and 2 different gRNAs targeting either *hey1* or *id2b* exons 1 and 2 (Figure 3-figure supplement 3a). These fish were raised to adults and gene deletions were confirmed using genomic DNA from fin clips (Figure 3-figure supplement 3e and f). Consistent with our MO-mediated knockdown experiments, only editing of the *hey1* gene resulted in increased injury-dependent MG proliferation and an expanded zone of injury-responsive MG (Figure 3f-h). Furthermore, this increased proliferation with Hey1 inactivation did not have a significant effect on retinal cell death (Figure 3-figure supplement 3g).

Although Hey1 inactivation appeared to lower MG's injury-response threshold, overexpression of either Hey1 or Id2b in *hsp70:GFP-P2A-hey1* and *hsp70:id2b-P2A-GFP* fish suppressed injury-dependent MG proliferation without affecting retinal cell death (Figure 3i; Figure 3-figure supplement 3h). Finally, Hey1 overexpression suppressed injury-dependent induction of regeneration-associated genes, like *ascl1a* and *lin28a* (Figure 3j). Together, the above data suggests Hey1 and Id2b inhibit injury-dependent proliferation of MG-derived progenitors, but only Hey1 regulates MG's injury response threshold.

Injury-dependent changes in Notch signaling component gene expression

We previously reported that *dll4* and *hey1* suppression correlates with Notch signaling suppression in the injured retina(Wan & Goldman 2017). Indeed, Hey1 appears to mediate the effects of Notch signaling on MG's injury response threshold (Figure 3). The correlation of *dll4* expression with that of *hey1* suggested Dll4 is a quiescence promoting factor. However, Dll4 was recently reported to stimulate proliferation of MG-derived progenitors in the injured retina(Campbell et al 2021). This inconsistency prompted us to reevaluate Notch signaling component gene expression in uninjured and injured retina.

We first investigated the relationship between Notch signaling component gene expression and MG quiescence. For this analysis, we interrogated previously generated RNAseq data sets that were obtained from GFP+ MG and GFP+ activated MG (2 dpi)(Lee et al 2020). This analysis indicated that *dll4* and *notch3* are more highly expressed in quiescent MG than any other Notch ligand/receptor encoding gene (Figure 4a). Importantly, these are the only Notch ligand/receptor encoding genes whose injury-dependent suppression is observed at 2 dpi when Notch signaling remains repressed (Figures 4a; Figure 4-figure supplement 4e)(Wan & Goldman 2017). In addition, PCR analysis of Notch signaling component gene expression using total retinal RNA revealed additional Notch ligand and receptor encoding genes that are transiently suppressed at early times post needle poke injury (Figure 4b; Figure 4-figure supplement 4a; Figure 4b-table supplement 6). Of these genes, *dll4*, *dlb,* and *notch3* were also shown to be suppressed in the light damaged retina(Campbell et al 2021).

Based on the above results, Dll4, Dlb, and Notch3 appeared to be good candidates for mediating Notch signaling and MG quiescence in the zebrafish retina. Indeed, Dlb expression in retinal neurons has been proposed to act via Notch3 to stimulate MG quiescence(Campbell et al 2021). However, as mentioned above, these same authors reported Dll4 expression stimulates MG proliferation in the injured retina. This result surprised us since, like *dlb*, *dll4* is repressed following retinal injury and its expression more closely follows that of Notch signaling than *dlb* (Figure 4a and b; Figure 4-figure supplement 4e). Although *dlb* was reported to be enriched in the retinal neuron population, a similar analysis of *dll4* was not performed. To further explore *dll4* expression in relation to *dlb* and *notch3*, we queried previously generated bulk RNAseq data sets from MG and nonMG and scRNAseq data sets from uninjured and injured retina(Hoang et al 2020). This analysis revealed that although *dlb* and *dll4* are generally expressed at low levels, *dll4* expression exceeds that of *dlb* in both MG and nonMG populations (Figure 4c). Furthermore, consistent with *in situ* hybridization assays(Campbell et al 2021), *notch3* is enriched in the MG population (Figure 4c). Interestingly, retinal injury suppressed *notch3* and *dll4* in both the MG and nonMG population, while *dlb* was less affected (Figure 4d). As controls, we evaluated *elavl3* and *ascl1a* expression - *elavl3* is an amacrine and ganglion cell marker, while *ascl1a* is a marker of activated and proliferating MG and MG-derived progenitors (Figure 4d).

To more carefully analyze the retinal cell types expressing these genes, we interrogated previously generated scRNAseq data sets from uninjured and injured retina(Hoang et al 2020). This analysis indicated *dlb* and *dll4* are expressed at low levels in MG, resulting in only a small fraction of MG showing expression above background (Figure 4e; Figure 4-figure supplement 4b). Nonetheless, in the uninjured

retina, *dlb* is enriched in progenitors and activated MG, while *dll4* predominates in the vascular endothelial (V/E) cell population (Figure 4e; Figure 4-figure supplement 4b). Both genes are poorly expressed in neurons; however, *dll4* expression exceeds that of *dlb* (Figure 4e; Figure 4-figure supplement 4b). Importantly, retinal injury rapidly reduced the population of V/E cells with detectable *dll4* expression, while *dlb* expression was reduced in activated MG (Figure 4e). In contrast to *dlb* and *dll4*, *notch3* expression is highest in the pericyte and MG population, and this MG expression is reduced after injury (Figure 4e). As expected, scRNAseq data sets show induction of *ascl1a* in activated MG following retinal injury, while *elavl3* expression is enriched in the amacrine (AC) and retinal ganglion cell (RGC) populations in both uninjured and injured retina (Figure 4e). The increased expression of *ascl1a* in resting MG after injury indicates that a fraction of these cells are transitioning to an activated state.

The above analysis raises the interesting possibility that neurodegeneration in the retina impacts V/E cells to control *dll4* expression. The relatively high expression of *dll4* in V/E cells and its coordinate repression with *notch3* in MG, suggests a mechanism for regulating Notch signaling in MG. Indeed, MG end feet are in direct contact with V/E cells(Alvarez et al 2007). Importantly, both photoreceptor degeneration in the light damaged retina and degeneration of amacrine and ganglion cells in the NMDA damaged retina reduce *dll4* expression in V/E cells(Hoang et al 2020). However, cell type-specific *dll4* and *dlb* gene knockdown or inactivation in MG, V/E cells, and neurons will be needed to identify the cell sources controlling Notch signaling in MG.

Notch signaling inhibits proliferation of MG-derived progenitors

Although the above data suggested Dll4 is a good candidate for engaging Notch3 receptors on MG and thus, maintaining MG quiescence, Dll4-dependent activation of Notch signaling was recently reported to stimulate proliferation of MG-derived progenitors(Campbell et al 2021). This result seemed at odds with Notch signaling being associated with quiescent MG as reported by nuclear localized mCherry expression in *tp1:mCherry* fish (Figure 4-figure supplement 4c)(Parsons et al 2009); its transient suppression in activated MG and MG-derived progenitors (Figure 4-figure supplement 4d and e); and a previous study reporting conditional expression of NICD at 3-4 dpi inhibited proliferation of MG-derived progenitors(Wan et al 2012). Although mCherry immunofluorescence indicates Notch signaling is repressed in proliferating MG and MG-derived progenitors, our qPCR analysis of retinal *mCherry* RNA suggests it returns by 4 dpi (Figure 4-figure supplement 4e). To further explore the relationship between Notch signaling and proliferation of MG-derived progenitors, we injured fish retinas with a needle poke and labelled proliferating cells at 2 dpi with an intraperitoneal (IP) injection of EdU. Fish were then

immersed in either DMSO or DAPT for an additional 2 days before receiving an IP injection of BrdU 3hrs prior to sacrifice. Quantification of the fraction of EdU+ cells that continued to proliferate at 4 dpi (BrdU+ & EdU+) revealed enhanced proliferation of MG-derived progenitors when Notch signaling was inhibited (Figure 4-figure supplement 4f). Thus, our data is most consistent with the idea that Notch signaling promotes quiescence of MG and MG-derived progenitors. Thus, the return of Notch signaling to the injured retina around 3-4 dpi (Figure 4-figure supplement 4e), which parallels the large increase in expression of Notch ligand encoding genes (Figure 4b; Figure 4-figure supplement 4a), likely facilitates progenitor cell cycle exit and differentiation.

Dlb, Dll4 and Notch3 regulate MG's response threshold to retinal injury

Our studies suggest Notch signaling regulates MG's injury response threshold and also the proliferation of MG-derived progenitors. MG's injury response threshold is reflected by the zone of proliferating MG responding to a needle poke injury(Wan et al 2012). A previous study suggested Dlb may be involved in regulating this injury response threshold since Dlb knockdown increased the number of MG that engage in a regenerative response in the light damaged retina(Campbell et al 2021). We obtained a similar result in the needle poke injured retina using a translation blocking MO that was validated in zebrafish embryos injected with a *dlb-GFP* chimeric transcript (Figure 5-figure supplement 5a-d). Following Dlb knockdown, we noted an expanded zone of proliferating MG (Figure 5-figure supplement 5b-d). Furthermore, Dlb overexpression in *hsp70:GFP-p2A-dlb* fish, inhibited injury-dependent proliferation of MG-derived progenitors (Figure 5-figure supplement 5f and g).

Although the above data may argue that Dlb maintains Notch signaling in quiescent MG, there are a few reasons to consider Dll4 as a candidate. First, basal levels of *dll4* in the uninjured retina exceed *dlb*, and its injury-dependent repression is greater than *dlb* (Figure 4); this is likely to translate into a more robust effect on Notch signaling levels. Second, the temporal aspect of *dll4* repression in the injured retina more closely mimics the changing levels of Notch signaling, while *dlb* repression is more transient and exceeds basal levels when Notch signaling activity is still low (Figure 4a and b; Figure 4-figure supplement 4a and e). Finally, *hey1* is a direct target of Notch signaling that regulates MG's injury response threshold (Figure 3), and we previously found that injury-dependent regulation of *hey1* expression correlates with that of *dll4*(Wan & Goldman 2017).

To investigate if Dll4 regulated MG's injury response threshold, we knocked down its expression using a *dll4*-MO that blocks *dll4* splicing and results in intron retention (*dll4*-MO, Figure 5a; Figure 5-figure

supplement 5h). Dll4 knockdown resulted in a dose-dependent increase in MG proliferation and an expanded zone of injury responsive proliferating MG (Figure 5b-d). Dll4 knockdown had no significant effect on retinal cell death (Figure 5e). Because this result contradicted a previous report(Campbell et al 2021), we used a CRISPR-based method to edit the *dll4* gene. For this analysis gRNAs were designed so they would target *dll4*'s DSL domain (gRNAs 1 and 2, Figure 5a), which is responsible for interacting with the Notch receptor extracellular domain. gRNAs were cloned into a Tol2 vector that allows expression of multiple gRNAs from different *u6* promoters(Yin et al 2015), and these fish were named *u6:dll4-gRNA$_{1,2}$*. These fish were bred with *ubi:Cas9* transgenic fish to generate *ubi:Cas9;u6:dll4-gRNA$_{1,2}$* fish. Fish harboring *dll4* gene deletions were identified by PCR using genomic DNA (Figure 5-figure supplement 5i). Like Dll4 knockdown, retinal injury in *ubi:Cas9;u6:dll4-gRNA$_{1,2}$* fish increased the number of MG engaged in a proliferative response, which was reflected by an expanded zone of injury-responsive proliferating MG (Figure 5f-h). CRISPR-mediated *dll4* gene editing had no significant effect on retinal cell death (Figure 5i). Finally, forced expression of Dll4 with heat shock in *hsp70:dll4-P2A-GFP* transgenic fish inhibited injury-dependent proliferation of MG-derived progenitors without affecting retinal cell death (Figure 5j-l; Figure 5-figure supplement 5j). Together, these data provide a strong case for Dll4 stimulating MG quiescence and regulating MG's injury response threshold. Furthermore, these experiments indicate that Dll4 expression inhibits proliferation of MG-derived progenitors.

We next investigated the consequences of Notch3 signaling on MG's injury response threshold. *In situ* hybridization assays and scRNAseq data indicate *notch3* is enriched in the MG population (Figure 4c)(Campbell et al 2021). In addition, *notch3* (*n3*) stands out from other Notch receptor encoding genes with relatively high basal expression, injury-dependent suppression (Figure 4a, b and e; Figure 4-figure supplement 4a), and enhanced MG proliferation with reduced expression in the light damaged retina(Campbell et al 2021). Consistent with this result, we found that Notch3 knockdown with a translation-blocking MO that successfully suppressed chimeric *notch3-GFP* RNA expression increased the number of MG recruited to a regenerative response as indicated by an expanded zone of injury-responsive MG (Figure 5-figure supplement 6a-e). This enhanced engagement of MG in an injury response was not accompanied by a change in dying neurons (Figure 5-figure supplement 6f). We confirmed this result using a CRISPR-based strategy to delete the *notch3* gene's ankyrin repeat domain that is required for recruiting MAML to the Rbpj-NICD complex (gRNA$_1$ and gRNA$_2$, Figure 5-figure supplement 6a and g)(Nam et al 2006). Retinal injury in *ubi:Cas9;u6:n3-gRNA$_{1,2}$* transgenic fish resulted in increased MG proliferation and an expanded zone of injury-responsive MG without any changes in

retinal cell death (Figure 5-figure supplement 6h-k). Together, the above results suggest that Dll4 and Dlb, acting through Notch3, regulate MG's quiescence and injury response threshold.

Epistasis experiments suggest bifurcation of Notch signaling via regulated expression of *hey1* and *id2b*

The above studies suggested Dll4 and Dlb engage the Notch3 receptor to stimulate Hey1 and Id2b expression and that these latter factors regulate MG quiescence and MG's injury response threshold. To further test this idea, we first investigated if Dll4 and Dlb required Notch3 to regulate these processes. Indeed, the normal suppression of MG proliferation and the reduced zone of proliferating MG resulting from Dll4 or Dlb overexpression was abrogated following Notch3 knockdown (Figure 6a and b).

We next investigated if Hey1 and Id2b acted downstream of these Notch signaling components. For this analysis we knocked down the expression of each of the Notch signaling components with and without Hey1 or Id2b overexpression in *hsp70:hey1-p2A-GFP* and *hsp70:Id2b-p2A-GFP* fish, respectively. Remarkably, Hey1 potently suppressed proliferation of MG and MG-derived progenitors, and dramatically reduced the zone of injury-responsive MG when Notch signaling components were knocked down (Figure 6c and d). In contrast, Id2b only reduced proliferation of MG-derived progenitors without any detectable effect on the zone of proliferating MG in retinas with Notch signaling component knockdown (Figure 6c and d).

Thus, our data are consistent with a Notch-Hey1 signaling pathway that regulates both MG's injury response threshold and the proliferation of MG-derived progenitors, while a Notch-Id2b signaling pathway appears to predominantly regulate proliferation of MG-derived progenitors. Thus, Hey1 and Id2b represent a point of bifurcation where downstream effectors have unique and overlapping consequence on retina regeneration.

Notch signaling regulation during development

We previously demonstrated that Notch signaling is restricted to quiescent MG in the adult zebrafish retina where it regulates MG's regenerative response(Elsaeidi et al 2018, Wan & Goldman 2017). In contrast, Notch signaling in the mouse retina is only transiently detected in postnatal MG and becomes undetectable in adults(Elsaeidi et al 2018, Nelson et al 2011). To compare this mammalian pattern of retinal Notch signaling during development with that of fish, we crossed *tp1:mCherry* Notch reporter fish with *gfap:GFP* fish that label MG (Kassen et al 2007, Parsons et al 2009). PCR analysis of *mCherry* and *gapdh*$_s$ expression in *tp1:mCherry;gfap:GFP* fish revealed reduced *mCherry* expression following immersion in DAPT-treated fish water, thus confirming their utility as a Notch signaling reporter (Figure

7-figure supplement 7a). In developing fish, mCherry and GFP immunofluorescence indicate Notch signaling is activated and restricted to differentiating MG within the first 2 days post-fertilization (dpf), preceding *gfap:GFP* transgene induction (Figure 7). mCherry immunofluorescence was not detect in progenitors residing in the retinal periphery. qPCR quantification of retinal *mCherry* RNA levels indicates a gradual reduction in Notch as the fish matures (Figure 7-figure supplement 7b). Nonetheless, unlike that of mouse MG, the remaining Notch signaling in adult zebrafish MG is readily detected and regulated by retinal injury, γ-secretase inhibitors, and DN-MAML (Figure 4-figure supplement 4c-f, Figure 7-figure supplement 7b)(Elsaeidi et al 2018, Wan & Goldman 2017). Thus, a major distinction between pro-regenerative MG in zebrafish and non-regenerative MG of mammals is the retention of Notch signaling in MG as they mature.

Discussion

In this paper we report on mechanisms by which Notch signaling regulates MG quiescence and stem cell activation in the zebrafish retina. We previously reported that Notch signaling is restricted to MG in the uninjured retina and rapidly suppressed in MG that engage in a regenerative response(Wan & Goldman 2017). Remarkably, pan-retinal inhibition of Notch signaling increases the number of MG that engage in a regenerative response. This is readily discerned in retinas with a needle poke injury where the zone of proliferating MG around the injury site is expanded following Notch inhibition(Wan et al 2012). This expansion suggests Notch regulates MG's injury response threshold allowing normally quiescent MG at a distance from the injury site to mount a regenerative response (Fig. 8). This scenario predicts a gradient of injury-derived factors that must exceed a certain level in order to engage MG in a regenerative response (Fig. 8). Indeed, this is reflected in studies showing relatively low levels of neuron death do not engage MG in an regenerative response(Iribarne et al 2019, Lessieur et al 2019, Montgomery et al 2010); and that the combination of Notch inhibition with intravitreal injection of the injury-related factor, Tnfa, increases the number of MG engaged in a regenerative response(Conner et al 2014).

Here we report that Notch raises MG's injury response threshold by regulating chromatin accessibility and the expression of a subset of regeneration-associated genes. Because Notch suppression in the uninjured retina generally stimulated MG chromatin compaction and gene expression, we reasoned an intervening repressor must be involved. Indeed, by intersecting MG RNAseq data sets that identify

injury-responsive genes with those that identify Notch-responsive genes, we were able to identify 2 candidate repressors, *hey1* and *id2b*. Remarkably, Hey1 increases MG's injury response threshold and also inhibits proliferation of MG-derived progenitors, while Id2b only inhibits the proliferation of MG-derived progenitors.

Hey1 is a member of the basic helix-loop-helix orange family of transcriptional repressors, while Id2b is a helix-loop-helix protein that lacks a DNA binding domain and sequesters basic helix-loop-helix proteins, like Ascl1a, from their target genes. Our finding that Hey1 acts downstream of Notch signaling to regulate MG's injury response threshold and proliferation is similar to that of brain radial glia where Notch signaling maintains neural stem cell quiescence and regulates proliferation of transient amplifying cells(Alunni et al 2013, Engler et al 2018, Imayoshi et al 2010, Kawai et al 2017, Than-Trong et al 2018). Furthermore, Hey1 can suppress expression of Ascl1 and Ascl1-regulated genes which is necessary for establishing a transient amplifying population of neural progenitors in the adult brain(Kim et al 2007, Sakamoto et al 2003). Importantly, Ascl1a is a pioneer transcription factor that can enhance chromatin accessibility across the genome and thereby influence the expression of many other genes(Wapinski et al 2017). Thus, the Notch-Hey1-Ascl1a signaling axis identified in zebrafish MG appears to be a conserved pathway in a variety of adult neural stem cell populations where it functions to control stem cell quiescence and progenitor amplification.

In both zebrafish and mice, Notch signaling is necessary for MG gene expression and differentiation(Bernardos et al 2005, Jadhav et al 2006, Nelson et al 2011, Scheer et al 2001). It has been suggested that release from Notch signaling is necessary for retinal progenitors to differentiate, and that reestablishment of Notch signaling in post mitotic progenitors stimulates MG differentiation(Jadhav et al 2006). Indeed, we show Notch signaling is restricted to MG in the developing and adult zebrafish retina(Wan & Goldman 2017). In contrast, Notch signaling is only transient in the developing mouse retina, being restricted to early postnatal stages when MG exhibit enhanced stem cell properties(Loffler et al 2015, Nelson et al 2011). Thus, one distinguishing feature of pro-regenerative MG is the maintenance of Notch signaling throughout life, which may allow them to retain stem cell features that facilitates their engagement in a regenerative response.

We previously reported that injury-dependent *dll4* suppression correlates with reduced Notch signaling and *hey1* expression in MG engaged in a regenerative response(Wan & Goldman 2017). Furthermore, *dll4* and *notch3* gene expression were the only Notch signaling components remaining repressed at 2 dpi when Notch signaling is repressed. Therefore, we wondered if Dll4 and Notch3 regulated MG's injury

response threshold. Indeed, either Dll4 or Notch3 inactivation using knockdown or CRISPR-based gene editing strategies resulted in an expanded zone of injury-responsive MG. Consistent with this result, restoration of Dll4 to MG in the injured retina using *hsp70:dll4-P2A-GFP* fish reduced proliferation of MG and MG-derived progenitors. Surprisingly, these results are inconsistent with a recent report indicating that Dll4 knockdown inhibits proliferation of MG and MG-derived progenitors(Campbell et al 2021). Although we do not know the reason for this discrepancy we note that this latter report relied solely on MO-mediated Dll4 knockdown to reach its conclusion. Furthermore, reduced Notch signaling that should accompany Dll4 knockdown is expected to stimulate MG proliferation(Conner et al 2014, Wan et al 2012), rather than inhibit it as reported by Campbell et al., 2020. Indeed, we show that inhibition of Notch signaling from 2-4 dpi stimulated proliferation of MG-derived progenitors.

Interestingly, Campbell et al., 2020 also reported that Dlb, acting via the Notch3 receptor, was responsible for maintaining MG quiescence in the uninjured retina. However, epistasis/rescue assays were not performed to lend credence to this supposition. We confirmed these results and also employed epistasis/rescue experiments to show Dll4 and Dlb act upstream of Notch3 to regulate MG's injury response threshold and proliferation of MG-derived progenitors. Furthermore, these experiments also indicated that Hey1 and Id2b act downstream of these Notch signaling components and represent a bifurcation in Notch signaling which differentially affect MG's injury response threshold.

Although Dll4 and Dlb stimulate Notch signaling in quiescent MG, the ligand presenting cell remains controversial. Both genes are detected at low levels in RNAseq data sets from MG purified from uninjured and injured (2 dpi) retinas(Lee et al 2020), and injury-dependent repression of *dll4* expression in MG more closely correlates with Notch signaling repression than does injury-dependent changes in *dlb* expression. *dlb* was previously reported to be enriched in the retinal neuron population(Campbell et al 2021); however, when we use the same RNAseq and scRNAseq data sets to compare *dll4* and *dlb* expression levels(Hoang et al 2020), we find *dll4* expression generally exceeds that of *dlb* in neurons. Importantly, these data indicate *dlb* is mostly expressed in activated MG and progenitor populations, while *dll4* is enriched in the V/E population. In addition, scRNAseq data sets from uninjured and injured retina indicated injury-dependent suppression of *dll4* in the MG, neuronal, and V/E cell populations, while *dlb* repression was restricted to the activated MG population. Injury-dependent regulation of *dll4* expression in V/E cells raises the interesting possibility that neuronal injury is communicated indirectly to MG via endothelial cells that make contact with MG end-feet. Indeed, rod loss has been associated with remodeling of the neurovascular unit, as are changes in neural activity(Attwell et al 2010, Garhofer

et al 2020, Ivanova et al 2019). However, without cell type-specific gene inactivation we cannot distinguish if Notch signaling in MG is regulated by Notch ligands expressed in neurons, endothelial cells, and/or MG.

In addition to their role in retina regeneration, Dll4 and Notch3 are required for angiogenesis and oligodendrocyte development, and loss of either gene is lethal(Leslie et al 2007, Zaucker et al 2013). Thus, one may wonder why the *ubi:Cas9*;*u6:dll4-gRNAs*$_{1,2}$ and *ubi:Cas9*;*u6:n3-gRNAs*$_{1,2}$ transgenic fish used in our studies survive to adulthood. We suspect mosaicism in CRISPR-mediated gene editing underlies this survival. This mosaicism may allow normal development to ensue; however, gene edits will continue to accumulate throughout the fish's life, which led to the noted enhanced regeneration phenotype in adult fish. We also note that although many homozygous *notch3* mutant fish do not survive to adulthood, some do(Zaucker et al 2013).

In summary, our studies have revealed a mechanism by which Notch signaling controls MG's injury response threshold and the proliferation of MG-derived progenitors. Our studies are consistent with Notch playing 3 roles in the retina: 1) Notch signaling may be required for MG to maintain stem cell characteristics and distinguishes pro-regenerative MG of fish from non-regenerative MG of mammals; 2) Notch acts via Hey1 to raise MG's injury-response threshold; thus, impacting the number of MG engaged in a regenerative response; and 3) Increasing delta ligand expression in proliferating MG-derived progenitors stimulates their cell cycle exit as they prepare to differentiate.

Materials and methods

Experimental models

Zebrafish: Animal studies were approved by the University of Michigan's Institutional Animal Care and Use Committee. Zebrafish were kept at 26-28°C with a 14/10 hr light/dark cycle. Adult male and female fish from 6 to 12 months of age were used in these studies. *1016 tuba1a:GFP*, *gfap:GFP*, *hsp70:DN-MAML-GFP, gfap:mCherry* and *tp1:mCherry*, fish were previously described(Fausett & Goldman 2006, Johnson et al 2016, Kassen et al 2007, Parsons et al 2009, Zhao et al 2014a). We generated *hsp70:dll4-P2A-GFP, hsp70:GFP-P2A-dlb, hsp70:GFP-P2A-hey1*, *hsp70:id2b-P2A-GFP, ubi:Cas9*, *u6:dll4-gRNAs*$_{1,2}$ and *u6:n3-gRNAs*$_{1,2}$ transgenic fish using standard recombinant DNA techniques and Tol2 vector backbone. Expression constructs were injected into single cell zebrafish embryos as previously described(Fausett & Goldman 2006). Fish were anesthetized in tricaine and retinas were injured with needle pokes (2-4

injuries/retina for analysis of proliferation and protein expression on retinal sections and 8 injuries/retina for qPCR, ATACseq and RNAseq), as previously described(Fausett & Goldman 2006).

Cell proliferation assays

To investigate cell proliferation, fish received an IP injection of EdU (10 μl of 10mg/ml stock) and Click-It chemistry was used for detection as previously described(Wan & Goldman 2017). Some fish received an IP injection of BrdU (20 mM).

RNA isolation and PCR

Total RNA was isolated using Trizol (Invitrogen). cDNA synthesis and PCR reactions were performed as previously described(Fausett et al 2008, Ramachandran et al 2010a). Real-time qPCR reactions were carried out using Green 2x LO-ROX qPCR mix (ASI) on an iCycler real-time PCR detection system (BioRad). The ΔΔCt method was used to determine relative expression of mRNAs in control and injured retinas and normalized to either *gapdh* or *gapdh$_s$* mRNA levels. Individual comparisons were done using unpaired 2-tailed Student t-test. ANOVA with Fisher's PLSD post hoc analysis was used for multiple parameter comparison. Error bars are standard deviation (SD).

ATACseq and RNAseq

For ATACseq and RNAseq, retinas from injured (2 dpi) *1016 tuba1a:GFP* and uninjured *gfap:GFP* fish were dissociated and GFP+ MG were purified using FACS in the University of Michigan's Cell Sorting Core as previously described(Powell et al 2013, Ramachandran et al 2010a). For ATACseq nuclei were isolated from GFP+ cells; transposase treatment and PCR amplification were as previously described(Buenrostro et al 2015). For RNAseq, RNA was purified from GFP+ cells and RNA quality and quantity analyzed on a Bioanalyzer (Agilent). cDNA libraries were generated by the U of M's Advance Genomics Core and DNA was sequenced on an Illumina NovaSeq 6000 platform. Sequencing reads were analyzed by the University of Michigan's Bioinformatics Core. The number of reads for each expressed gene was determined and differentially expressed genes were restricted to those exhibiting at least a 1.5-fold difference in expression with threshold abundance greater than 5 Fragments Per Kilobase of transcript per Million mapped reads to eliminate very low abundant transcripts whose estimates of fold-change are unreliable.

Bulk RNA-seq data analysis of MG and nonMG

MG RNAseq data generated from *gfap:GFP* transgenic fish treated +/- NMDA, and light damaged fish retinas were obtained from Hoang et al., 2020. The original raw sequencing reads were processed by the authors as described(Hoang et al 2020). Briefly, RNAseq libraries were prepared from FACS purified MG and nonMG with a result of 45 to 55 million reads per library. Each condition contained two biological replicates, and FPKM (fragments per kilobase of exon per million) were calculated using the raw counts of genes. Using this dataset, we identified genes of interest and the corresponding FPKM across samples were averaged and formulated into heat maps using R for visualization.

scRNAseq data analysis of control and NMDA-treated retinas

Retinal scRNAseq data from control and NMDA damaged fish retinas were obtained from Hoang et al., 2020. Briefly, the authors used Cell Ranger from 10x Genomics to map zebrafish reads from scRNAseq to the genome with an average of 1000 to 1500 genes and 2500 to 3250 unique molecular identifiers per cell. Variable genes were identified and clustered with K-nearest neighbors and shared nearest neighbor modularity optimization through Seurat. Doublets were eliminated with an in-house algorithm, and marker genes were used to annotate cell types for each cell cluster identified. Using this dataset, we identified the scaled and normalized average expression of our genes of interest across cell clusters, and the percentage of cells per cluster expressing these genes were calculated using R. Dot plots were created using Seurat for visualization.

CRISPR-based gene editing

Gene editing was performed as previously described(Hwang et al 2013, Vejnar et al 2016). Briefly, we used CRISPRscan to identify 3-6 gRNAs that target the gene of interest(Moreno-Mateos et al 2015). gRNA DNA template synthesis using gRNA primer, universal primer, and *in vitro* transcription are as previously described(Vejnar et al 2016). gRNAs are tested for editing efficiency by injecting single cell embryos with *in vitro* transcribed gRNA, along with Cas9-nanos RNA; 2-4 days later, editing efficiency is determined using genomic DNA in T7 endonuclease 1 (T7E1) mismatch detection assays and PCR(Sentmanat et al 2018). For stable gene editing in transgenic fish, we generated *Ubi:Cas9;cmlc2:GFP* (*Ubi:Cas9*) transgenic fish using standard recombinant DNA protocols and Tol2 vectors. We also generated Tol2 vectors harboring two gRNAs targeting a single gene under the control of two *u6a* promoters as previously described(Yin et al 2015). We chose to express 2 gRNAs for each gene to improve editing efficiency and generate large deletions. Stable transgenic lines were established as previously described and are referred to as *u6:gene-gRNA*$_{1,2}$(Fausett & Goldman 2006). For gene editing

in transgenic lines, *Ubi:Cas9* fish and *u6:gene-gRNA$_{1,2}$* were bred to each other and *Ubi:Cas9;u6:gene-gRNA$_{1,2}$* fish (F1 generation) were used for gene editing experiments. Gene editing in transgenic fish was confirmed by PCR and DNA sequencing. For gene editing in F0 fish, we injected zebrafish embryos with previously validated *in vitro* transcribed gRNAs$_{1,2}$ and *Cas9-nanos* mRNA. Embryos were raised to adults and genomic DNA from fin clips was used in T7E1 mismatch detection assay and PCR to confirm gene editing(Sentmanat et al 2018).

MOs, gRNAs, and qPCR Primers used in this study

All MOs, gRNAs, and primers used in this study are listed in Table Supplement 7.

Morpholino (MO) functional assays

MOs were obtained from Gene Tools, LLC and the sequences are listed in Supplementary Table 7. All MOs have a lissamine tag. Unless otherwise stated, MOs were used at 1 mM concentration. For testing splice blocking *dll4*-and *hey1*-targeting MO, we injected either control MO or experimental MO (~1ng) into single cell zebrafish embryos. RNA was extracted from embryos at 24-48hrs post injection and assayed for *dll4* or *hey1* mRNA by PCR. For testing *dlb-*, *n3-*, and *id2b*-targeting MOs, we generated *pCS2+dlb-EGFP*, *pCS2+n3-EGFP* and *pCS2+id2b-EGFP* constructs that contained either *dlb*, *n3*, or *id2b* MO target site upstream of the EGFP initiator AUG. Plasmids were linearized with Not1 restriction enzyme and capped sense RNA was synthesized using SP6 RNA polymerase using Invitrogen's mMESSAGE mMACHINE™ SP6 Transcription Kit (Invitrogen, #AM1340) according to manufactures directions. Following purification, the capped RNA was dissolved in nuclease free water containing 0.2% phenol red and injected with experimental or control MO into single cell zebrafish embryos. Each embryo received approximately 50 pg of RNA and 250 pg of control or experimental MO. MO's were delivered to adult fish via intravitreal injection at the time of retinal injury and cellular uptake was facilitated by electroporation as previously described(Fausett et al 2008).

Luciferase assay

A 3kb region upstream of the *hey1* gene's transcription start site was amplified by PCR and cloned into Xho1/Kpn1 sites of the *pXP1* plasmid to create *3kb-hey1:luciferase*. Using Q5® Site-Directed Mutagenesis Kit (NEB, E0554), we generated mutations in each of the two most highly conserved Rbpj binding sites (m1 and m2, Fig. 7a). Mutations were confirmed by DNA sequencing. To study *hey1* promoter activity, we transfected HEK 293T cells plated in 24 well tissue culture plates with wt and mutant *3kb-hey1:luciferase*, +/- CMV:NICD and *SV40:Renilla* as internal control using lipofectamine 3000

(Invitrogen). Two days after transfection, cells were washed with PBS, lysed, and luciferase and Renilla activities measured using a Luminometer (Turner Biosystems). Luciferase activity was normalized to Renilla activity.

Heat shock and pharmacological inhibitors

For heat shock, fish were immersed in a water bath at 37°C for 1 hr before returning to system water at 28°C. For extended periods of heat shock, this was repeated every 6 hrs. To inhibit Notch signaling we used DAPT (Cayman, Cat # 13197) prepared in DMSO as a 10mM stock and diluted 1/250 in fish water for immersion. Control fish were treated with vehicle. Fish were exposed to DAPT for 24 hours.

Immunofluorescence and TUNEL assay

Zebrafish samples were prepared for immunofluorescence as previously described(Fausett & Goldman 2006, Ramachandran et al 2010a, Ramachandran 2010). Primary antibodies used in this study: Rabbit anti-GFP, Thermo Fisher, Cat. # A6455 (1/1000); Mouse anti-mCherry, Abcam, Cat. # ab125096 (1:500); and mouse anti-glutamine synthetase (GS), Sigma-Aldrich, Cat. #MAB302 (1/500). Secondary antibodies used were: Alexa Flour 555 Donkey anti Mouse-IgG (H+L), Thermo Fisher Cat. # A31570 (1:500); Alexa flour 555 Donkey anti Rabbit IgG (H+L), Thermo Fisher, Cat # A31572 (1:500); Alexa Flour 488 donkey anti mouse Thermo Fisher Cat. # A21202 (1:500); Alexa Flour 488 goat anti rabbit Thermo Fisher Cat. # A11008 (1:500).

We used an *in situ* Cell Death Fluorescein Kit (Millipore Sigma, Cat. # 11684795910) to detect cells undergoing apoptosis.

Microscopy and cell quantification

Images were captured by a Zeiss Axiophot fluorescence microscope or a Leica DM2500 microscope. EdU and BrdU labelling were used to identify and quantify proliferating cells in retinal sections as previously described(Fausett & Goldman 2006, Ramachandran et al 2010a, Wan & Goldman 2017, Wan et al 2012, Wan et al 2014). The width of the proliferative zone was quantified at the center of the injury site where the largest number of proliferating cells reside.

Statistical analysis

Unless otherwise indicated, sample size is 3 fish and experiments were repeated at least 3 times. Statistical analyses were performed in GraphPad Prism. Error bars are standard deviation (SD). Two-

tailed Student's *t* test was used for single parameter comparison; all measurements were taken from distinct samples.

Data sharing

Raw data have been deposited in GEO under the superset accession number GSE160179 and will be released upon acceptance of manuscript for publication.

Acknowledgments

This work was supported by grants from the NIH (NEI RO1 EY018132 and NEI RO1 EY027310) and the Gilbert Family Foundation Vision Restoration Initiative. We thank David Hyde, Notre Dame, for *gfap:GFP* transgenic fish; Michael Parsons, University California, Irvine, for *tp1:mCherry* transgenic fish; Mi-Sun Lee for generating *ubi:Cas9* transgenic fish; Elizabeth Mills for generating *u6:dll4-gRNAs*$_{1,2}$ and *u6:n3-gRNAs*$_{1,2}$ transgenic fish; Muchu Zhou and Zachary Rekowski for maintaining our zebrafish colony; and all members of the Goldman lab for their comments on this work. We also acknowledge and thank the University of Michigan's Cell Sorting Core, Advanced Genomics Core, and Bioinformatics Core.

References

Alunni A, Krecsmarik M, Bosco A, Galant S, Pan L, et al. 2013. Notch3 signaling gates cell cycle entry and limits neural stem cell amplification in the adult pallium. *Development* 140: 3335-47

Alvarez Y, Cederlund ML, Cottell DC, Bill BR, Ekker SC, et al. 2007. Genetic determinants of hyaloid and retinal vasculature in zebrafish. *BMC Dev Biol* 7: 114

Attwell D, Buchan AM, Charpak S, Lauritzen M, Macvicar BA, Newman EA. 2010. Glial and neuronal control of brain blood flow. *Nature* 468: 232-43

Bernardos RL, Lentz SI, Wolfe MS, Raymond PA. 2005. Notch-Delta signaling is required for spatial patterning and Muller glia differentiation in the zebrafish retina. *Dev Biol* 278: 381-95

Buenrostro JD, Wu B, Chang HY, Greenleaf WJ. 2015. ATAC-seq: A Method for Assaying Chromatin Accessibility Genome-Wide. *Curr Protoc Mol Biol* 109: 21.29.1-21.29.9

Campbell LJ, Hobgood JS, Jia M, Boyd P, Hipp RI, Hyde DR. 2021. Notch3 and DeltaB maintain Muller glia quiescence and act as negative regulators of regeneration in the light-damaged zebrafish retina. *Glia* 69: 546-66

Conner C, Ackerman KM, Lahne M, Hobgood JS, Hyde DR. 2014. Repressing notch signaling and expressing TNFalpha are sufficient to mimic retinal regeneration by inducing Muller glial proliferation to generate committed progenitor cells. *J Neurocsci* 34: 14403-19

Elsaeidi F, Macpherson P, Mills EA, Jui J, Flannery JG, Goldman D. 2018. Notch Suppression Collaborates with Ascl1 and Lin28 to Unleash a Regenerative Response in Fish Retina, But Not in Mice. *J Neurosci* 38: 2246-61

Engler A, Zhang R, Taylor V. 2018. Notch and Neurogenesis. *Adv Exp Med Biol* 1066: 223-34

Fausett BV, Goldman D. 2006. A role for alpha1 tubulin-expressing Muller glia in regeneration of the injured zebrafish retina. *J Neurosci* 26: 6303-13

Fausett BV, Gumerson JD, Goldman D. 2008. The proneural basic helix-loop-helix gene ascl1a is required for retina regeneration. *J Neurosci* 28: 1109-17

Garhofer G, Chua J, Tan B, Wong D, Schmidl D, Schmetterer L. 2020. Retinal Neurovascular Coupling in Diabetes. *J Clin Med* 9: 2829

Goldman D. 2014. Muller glial cell reprogramming and retina regeneration. *Nature reviews. Neuroscience* 15: 431-42

Gorsuch RA, Lahne M, Yarka CE, Petravick ME, Li J, Hyde DR. 2017. Sox2 regulates Muller glia reprogramming and proliferation in the regenerating zebrafish retina via Lin28 and Ascl1a. *Exp Eye Res* 161: 174-92

Hoang T, Wang J, Boyd P, Wang F, Santiago C, et al. 2020. Gene regulatory networks controlling vertebrate retinal regeneration. *Science* 370: eabb8598

Hwang WY, Fu Y, Reyon D, Maeder ML, Tsai SQ, et al. 2013. Efficient genome editing in zebrafish using a CRISPR-Cas system. *Nat Biotechnol* 31: 227-9

Imayoshi I, Sakamoto M, Yamaguchi M, Mori K, Kageyama R. 2010. Essential roles of Notch signaling in maintenance of neural stem cells in developing and adult brains. *J Neurosci* 30: 3489-98

Iribarne M, Hyde DR, Masai I. 2019. TNFalpha Induces Muller Glia to Transition From Non-proliferative Gliosis to a Regenerative Response in Mutant Zebrafish Presenting Chronic Photoreceptor Degeneration. *Front Cell Dev Biol* 7: 296

Ivanova E, Alam NM, Prusky GT, Sagdullaev BT. 2019. Blood-retina barrier failure and vision loss in neuron-specific degeneration. *JCI Insight* 4: e126747

Jadhav AP, Cho SH, Cepko CL. 2006. Notch activity permits retinal cells to progress through multiple progenitor states and acquire a stem cell property. *Proc Natl Acad Sci U S A* 103: 18998-9003

Johnson K, Barragan J, Bashiruddin S, Smith CJ, Tyrrell C, et al. 2016. Gfap-positive radial glial cells are an essential progenitor population for later-born neurons and glia in the zebrafish spinal cord. *Glia* 64: 1170-89

Kassen SC, Ramanan V, Montgomery JE, C TB, Liu CG, et al. 2007. Time course analysis of gene expression during light-induced photoreceptor cell death and regeneration in albino zebrafish. *Dev Neurobiol* 67: 1009-31

Kawai H, Kawaguchi D, Kuebrich BD, Kitamoto T, Yamaguchi M, et al. 2017. Area-Specific Regulation of Quiescent Neural Stem Cells by Notch3 in the Adult Mouse Subependymal Zone. *J Neurosci* 37: 11867-80

Kim EJ, Leung CT, Reed RR, Johnson JE. 2007. In vivo analysis of Ascl1 defined progenitors reveals distinct developmental dynamics during adult neurogenesis and gliogenesis. *J Neurosci* 27: 12764-74

Lahne M, Nagashima M, Hyde DR, Hitchcock PF. 2020. Reprogramming Muller Glia to Regenerate Retinal Neurons. *Annu Rev Vis Sci* 6: 171-93

Lee MS, Wan J, Goldman D. 2020. Tgfb3 collaborates with PP2A and notch signaling pathways to inhibit retina regeneration. *Elife* 9: e55137

Lenkowski JR, Raymond PA. 2014. Muller glia: Stem cells for generation and regeneration of retinal neurons in teleost fish. *Progress in retinal and eye research* 40: 94-123

Leslie JD, Ariza-McNaughton L, Bermange AL, McAdow R, Johnson SL, Lewis J. 2007. Endothelial signalling by the Notch ligand Delta-like 4 restricts angiogenesis. *Development* 134: 839-44

Lessieur EM, Song P, Nivar GC, Piccillo EM, Fogerty J, et al. 2019. Ciliary genes arl13b, ahi1 and cc2d2a differentially modify expression of visual acuity phenotypes but do not enhance retinal degeneration due to mutation of cep290 in zebrafish. *PLoS One* 14: e0213960

Loffler K, Schafer P, Volkner M, Holdt T, Karl MO. 2015. Age-dependent Muller glia neurogenic competence in the mouse retina. *Glia* 63: 1809-24

MacDonald RB, Randlett O, Oswald J, Yoshimatsu T, Franze K, Harris WA. 2015. Muller glia provide essential tensile strength to the developing retina. *J Cell Biol* 210: 1075-83

Maillard I, Tu L, Sambandam A, Yashiro-Ohtani Y, Millholland J, et al. 2006. The requirement for Notch signaling at the beta-selection checkpoint in vivo is absolute and independent of the pre-T cell receptor. *J Exp Med* 203: 2239-45

Maillard I, Weng AP, Carpenter AC, Rodriguez CG, Sai H, et al. 2004. Mastermind critically regulates Notch-mediated lymphoid cell fate decisions. *Blood* 104: 1696-702

Montgomery JE, Parsons MJ, Hyde DR. 2010. A novel model of retinal ablation demonstrates that the extent of rod cell death regulates the origin of the regenerated zebrafish rod photoreceptors. *J Comp Neurol* 518: 800-14

Moreno-Mateos MA, Vejnar CE, Beaudoin JD, Fernandez JP, Mis EK, et al. 2015. CRISPRscan: designing highly efficient sgRNAs for CRISPR-Cas9 targeting in vivo. *Nat Methods* 12: 982-8

Nagashima M, Barthel LK, Raymond PA. 2013. A self-renewing division of zebrafish Muller glial cells generates neuronal progenitors that require N-cadherin to regenerate retinal neurons. *Development* 140: 4510-21

Nam Y, Sliz P, Song L, Aster JC, Blacklow SC. 2006. Structural basis for cooperativity in recruitment of MAML coactivators to Notch transcription complexes. *Cell* 124: 973-83

Nelson BR, Ueki Y, Reardon S, Karl MO, Georgi S, et al. 2011. Genome-wide analysis of Muller glial differentiation reveals a requirement for Notch signaling in postmitotic cells to maintain the glial fate. *PLoS One* 6: e22817

Parsons MJ, Pisharath H, Yusuff S, Moore JC, Siekmann AF, et al. 2009. Notch-responsive cells initiate the secondary transition in larval zebrafish pancreas. *Mech Dev* 126: 898-912

Powell C, Grant AR, Cornblath E, Goldman D. 2013. Analysis of DNA methylation reveals a partial reprogramming of the Muller glia genome during retina regeneration. *Proc Natl Acad Sci U S A* 110: 19814-9

Ramachandran R, Fausett BV, Goldman D. 2010a. Ascl1a regulates Muller glia dedifferentiation and retinal regeneration through a Lin-28-dependent, let-7 microRNA signalling pathway. *Nat Cell Biol* 12: 1101-7

Ramachandran R, Reifler, A., Parent, J.M and Goldman, D. 2010. Conditional gene expression and lineage tracing of tuba1a expressing cells during zebrafish development and retina regeneration. *J Comp Neurol* 518: 4196-212

Ramachandran R, Zhao XF, Goldman D. 2011. Ascl1a/Dkk/{beta}-catenin signaling pathway is necessary and glycogen synthase kinase-3{beta} inhibition is sufficient for zebrafish retina regeneration. *Proc Natl Acad Sci U S A* 108: 15858-63

Ramachandran R, Zhao XF, Goldman D. 2012. Insm1a-mediated gene repression is essential for the formation and differentiation of Muller glia-derived progenitors in the injured retina. *Nat Cell Biol* 14: 1013-23

Reichenbach A, Bringmann A. 2013. New functions of Muller cells. *Glia* 61: 651-78

Sakamoto M, Hirata H, Ohtsuka T, Bessho Y, Kageyama R. 2003. The basic helix-loop-helix genes Hesr1/Hey1 and Hesr2/Hey2 regulate maintenance of neural precursor cells in the brain. *J Biol Chem* 278: 44808-15

Scheer N, Groth A, Hans S, Campos-Ortega JA. 2001. An instructive function for Notch in promoting gliogenesis in the zebrafish retina. *Development* 128: 1099-107
Sentmanat MF, Peters ST, Florian CP, Connelly JP, Pruett-Miller SM. 2018. A Survey of Validation Strategies for CRISPR-Cas9 Editing. *Sci Rep* 8: 888
Sifuentes CJ, Kim JW, Swaroop A, Raymond PA. 2016. Rapid, Dynamic Activation of Muller Glial Stem Cell Responses in Zebrafish. *Invest Ophthalmol Vis Sci* 57: 5148-60
Than-Trong E, Ortica-Gatti S, Mella S, Nepal C, Alunni A, Bally-Cuif L. 2018. Neural stem cell quiescence and stemness are molecularly distinct outputs of the Notch3 signalling cascade in the vertebrate adult brain. *Development* 145: dev161034
Thomas JL, Ranski AH, Morgan GW, Thummel R. 2016. Reactive gliosis in the adult zebrafish retina. *Exp Eye Res* 143: 98-109
Vejnar CE, Moreno-Mateos MA, Cifuentes D, Bazzini AA, Giraldez AJ. 2016. Optimized CRISPR-Cas9 System for Genome Editing in Zebrafish. *Cold Spring Harb Protoc* 2016: doi:10.1101/pdb.prot086850
Wan J, Goldman D. 2016. Retina regeneration in zebrafish. *Curr Opin Genet Dev* 40: 41-47
Wan J, Goldman D. 2017. Opposing Actions of Fgf8a on Notch Signaling Distinguish Two Muller Glial Cell Populations that Contribute to Retina Growth and Regeneration. *Cell Rep* 19: 849-62
Wan J, Ramachandran R, Goldman D. 2012. HB-EGF is necessary and sufficient for Muller glia dedifferentiation and retina regeneration. *Dev Cell* 22: 334-47
Wan J, Zhao XF, Vojtek A, Goldman D. 2014. Retinal Injury, Growth Factors, and Cytokines Converge on beta-Catenin and pStat3 Signaling to Stimulate Retina Regeneration. *Cell Reports* 9: 285-97
Wapinski OL, Lee QY, Chen AC, Li R, Corces MR, et al. 2017. Rapid Chromatin Switch in the Direct Reprogramming of Fibroblasts to Neurons. *Cell Rep* 20: 3236-47
Xia W. 2019. gamma-Secretase and its modulators: Twenty years and beyond. *Neurosci Lett* 701: 162-69
Yin L, Maddison LA, Li M, Kara N, LaFave MC, et al. 2015. Multiplex Conditional Mutagenesis Using Transgenic Expression of Cas9 and sgRNAs. *Genetics* 200: 431-41
Zaucker A, Mercurio S, Sternheim N, Talbot WS, Marlow FL. 2013. notch3 is essential for oligodendrocyte development and vascular integrity in zebrafish. *Dis Model Mech* 6: 1246-59
Zhao L, Borikova AL, Ben-Yair R, Guner-Ataman B, MacRae CA, et al. 2014a. Notch signaling regulates cardiomyocyte proliferation during zebrafish heart regeneration. *Proc Natl Acad Sci U S A* 111: 1403-8
Zhao XF, Wan J, Powell C, Ramachandran R, Myers MG, Jr., Goldman D. 2014b. Leptin and IL-6 Family Cytokines Synergize to Stimulate Muller Glia Reprogramming and Retina Regeneration. *Cell Reports* 9: 272-84

Author contributions

AS designed and performed all experiments except ATACseq and generation of CRISPR gene edited fish. SD performed ATACseq experiments and generated CRISPR gene edited fish. JJ analyzed bulk RNAseq and scRNAseq data and helped in transfections. DG conceived, designed, and supervised the work and

co-wrote the manuscript and helped generate transgenic fish. All authors reviewed and edited the manuscript.

Figure legends

Figure 1: Injury-dependent regulation of MG gene expression and chromatin accessibility. a, MA plot of RNAseq data using MG purified from uninjured and injured fish retinas. **b**, qPCR analysis of select injury-regulated genes. **c**, Volcano plot of ATACseq data using MG purified from uninjured and injured fish retinas. **d**, Intersection of regeneration-associated genes with those whose chromatin accessibility changes with injury.

Figure 2: Notch-dependent regulation of MG gene expression and chromatin accessibility in uninjured retina. a, MA plot of RNAseq data from MG of uninjured fish treated +/- DAPT. **b**, Intersection of regeneration-associated genes with DAPT-regulated genes. **c**, Volcano plot of ATACseq data from MG of uninjured fish treated +/- DAPT. **d**, Intersection of regeneration-associated genes with those whose chromatin accessibility changes with DAPT treatment.

Figure 3: Hey1 and Id2b regulate MG's regenerative response. a, Illustration of *hey1* gene promoter from human, mouse and zebrafish with Rbpj binding sites indicated. **b**, Luciferase assays for Notch (NICD) dependent activation of Wt and mutant *hey1* promoter activity; Compared to Wt alone, ***P<0.0001. **c**, **f**, EdU Click-iT chemistry on retinal sections identifies proliferating cells in Wt fish treated with indicated MOs (**c**) or Cas9 and indicated gRNAs (**f**). **d**, **g**, **i**, Quantification of the number of EdU+ cells at 4 dpi; (**d**)***P=0.0008, (**g**) ***P<0.0001, (**i**) ***P<0.0001. **e**, **h**, Quantification of the width of the proliferative zone in retinas at 4 dpi; (**e**) ***P<0.0001, (**h**) ***P=0.0004. **j**, PCR analysis of the effects Hey1 expression has on injury-dependent induction of *ascl1a* and *lin28a*. Abbreviations: MO,

morpholino; C-MO or Con-MO, control-MO; ONL, outer nuclear layer; INL, inner nuclear layer; GCL, ganglion cell layer; Wt, wild type; m, mutant. Scale bars are 100 μm.

Figure 4: Analysis of Notch ligand and receptor gene expression in the uninjured and injured zebrafish retina. a, Expression level of indicated RNAs based on bulk RNAseq data generated from GFP+ MG FACS purified from uninjured *gfap:GFP* and GFP+ activated MG and MG-derived progenitors FACS purified from injured (2 dpi) *1016 tuba1a:GFP* fish(Lee et al 2020). **b**, qPCR heat map illustrating temporal changes in the expression of Notch ligand and receptor encoding genes at various times post needle poke injury. **c**, Expression level of indicated RNAs in MG and nonMG based on bulk RNAseq data generated by Hoang et al., 2020 using GFP+ MG and GFP- nonMG FACS purified from uninjured *gfap:GFP* fish. **d**, Temporal changes in indicated genes at various times post light damage based on bulk RNAseq data generated by Hoang et al., 2020 using GFP+ MG and GFP- nonMG FACS purified from injured *gfap:GFP* fish. **e**, Dot plot visualization of gene expression across retinal cell types in the uninjured and NMDA injured retina based on scRNAseq data from Hoang et al., 2020. Abbreviations: j, jag; n, notch; hpi, hours post injury; dpi, days post injury; FPKM, Fragments Per Kilobase of transcript per Million mapped reads.

Figure 5: Dll4 regulates MG's injury response threshold and proliferation of MG-derived progenitors. a, Diagram of the *dll4* gene with MO and gRNA target sites indicated. **b, f, j,** Fluorescent images showing EdU Click-iT chemistry on retinal sections at 4 dpi. **c, g, k,** Quantification of the number of EdU+ cells at 4 dpi; (**c**), compared to C-MO*P=0.0351 (0.2mM), **P=0.0022 (0.5mM), ***P=0.0003 (1mM); (**g**), compared to Cas9 ***P<0.0001; (**k**), ***P<0.0001. **d, h,** Quantification of the width of the proliferative zone in retinas at 4 dpi; (**d**), ***P<0.0001; (**h**), ***P<0.0001. **e, i, l,** Quantification of TUNEL+ cells at 1 dpi. Abbreviations: Wt, wild type; MO, morpholino; C-MO or Con-MO, control-MO; ONL, outer nuclear layer; INL, inner nuclear layer; GCL, ganglion cell layer. Scale bars are 100 μm.

Figure 6: Dll4 and Dlb engage the Notch3 receptor to induce Hey1 and Id2b expression and control retina regeneration. **a, c**, Quantification of proliferating MG-derived progenitors in the needle poke injured retina (2 dpi). **b**, **d**, Quantification of the zone of proliferating MG. (**a**), Compared to (C-MO, Wt), ***P=0.0003 C-MO, Dll4); **P=0.0011 (C-MO, Dlb); ***P<0.0001 (notch3-MO, Wt); ***P=0.0009 (notch3-MO, Dll4); **P=0.0022 (notch3-MO, Dlb). (**b**), Compared to (C-MO, Wt), **P=0.0014 (C-MO, Dll4); *P=0.0218 (C-MO, Dlb); **P=0.0031 (notch3-MO, Wt); *P=0.0197 (notch3-MO, Dll4); *P=0.0394 (notch3-MO, Dlb). (**c**), Compared to control MO (Con) in Wt retina, ***P<0.0001 (Wt, dll4-MO); ***P=0.0003 (Wt, dlb-MO); ***P<0.0001 (Wt, n3-MO); ***P=0.0003 (Hey1, Con-MO); ***P<0.0001 (Hey1, dll4-MO); ***P=0.0001 (Hey1, dlb-MO); ***P=0.0001 (Hey1, n3-MO); *P=0.0348 (Id2b, Con-MO); ***P=0.0006 (Id2b, dl4-MO); **P=0.0027 (Id2b, dlb-MO); ***P<0.0001 (Id2b, n3-MO). (**d**), Compared to control MO (Con) in Wt retina, ***P<0.0001 (Wt, dll4-MO); **P=0.0056 (Wt, dlb-MO); ***P<0.0001 (Wt, n3-MO); **P=0.0042 (Hey1, Con-MO); *P=0.0228 (Hey1, dll4-MO); *P=0.0132 (Hey1, dlb-MO); **P=0.0025 (Hey1, n3-MO); ***P=0.0004 (Id2b, dll4-MO); *P=0.021 (Id2b, dlb-MO); ***P=0.0002 (Id2b, n3-MO). Abbreviations: Wt, wild type fish; MO, morpholino; C-MO or con, control MO; n3, notch3; ns, not significant.

Figure 7: Notch signaling in the developing retina. GFP and mCherry immunofluorescence on retinal sections from *tp1:mCherry;gfap:GFP* transgenic fish at different times post fertilization. Dashed oval identifies retinal periphery where retinal stem cells involved in retinal expansion reside. Abbreviations: ONL, outer nuclear layer; INL, inner nuclear layer; GCL, ganglion cell layer. Scale bar is 50 μm. Abbreviations: ONL, outer nuclear layer; INL, inner nuclear layer; GCL, ganglion cell layer; dpf, day post fertilization.

Figure 8: Model illustrating the impact Notch signaling has on MG's regenerative response. **a**, Diagram of the effect of Notch signaling on MG gene expression and chromatin accessibility. Potential retinal cell

sources of Dll4 and Dlb are listed. **b**, Illustration of the effect Notch signaling has on MG's threshold response to injury-derived factors.

SUPPLEMENTARY FIGURE LEGENDS

Figure 1-figure supplement 1: Injury-regulated genes and chromatin accessibility. **a**, PCR and agarose gel analysis of select regeneration-associated genes at various times post injury. **b**, RNAseq FPKM values for select MG identity genes; ***P*=0.0029 (*glula*); ****P*=0.0004 (*rlbp1a*); ***P*=0.0048 (*sox2*); ***P*=0.001 (*gfap*); **P*=0.0198 (*apoeb*); ***P*=0.0017 (*fabp7a*). **c**, Annotation of injury-regulated ATACseq data to different genic features. **d**, Select ATACseq genomic tracts generated from GFP+ MG FACS purified from uninjured and needle poke injured *gfap:GFP* retinas.

Figure 2-figure supplement 2: Notch-regulated genes and chromatin accessibility. **a**, Top 20 injury-responsive genes that are also regulated in a similar direction by DAPT-treatment. **b**, qPCR time course analysis of select DAPT-regulated genes in the uninjured retina. **c**, RNAseq FPKM values for select MG identity genes; **P*=0.0385 (*gfap*). **d**, Annotation of DAPT-regulated ATACseq data to different genic features. **e**, Select ATACseq genomic tracts using GFP+ MG purified from uninjured *gfap:GFP* retinas treated +/-DAPT. **f**, Volcano plot of MG RNAseq data from *gfap:mCherry* and *gfap:mCherrry;hsp70:DN-MAML* heat shock treated fish.

Figure 3-figure supplement 3: Hey1 and Id2b regulate retina regeneration. **a**, Illustration of the *hey1* gene with MO and gRNA target sites indicated. **b**, PCR analysis of *hey1*-MO treatment stimulating *hey1* intron retention. **c**, *id2b*-MO suppressed *id2b-GFP* chimeric RNA expression in zebrafish embryos. Numbers in panels refer to number of lissamine+ fish with GFP+ phenotype. **d**, Quantification of EdU+ cells using Click-iT chemistry in *hey1*-MO treated retina; ***P*=0.0054 (0.2mM); ****P*=0.0002 (0.5mM); ****P*=0.0008 (1.0mM). **e**, **f**, Single cell embryos were injected with Cas9 RNA and the indicated gRNAs

and raised to adults. Shown is PCR analysis of genomic DNA from fin clips of adult fish. **g**, **h**, Quantification of TUNEL+ cells in the injured retina.

Figure 4-figure supplement 4: Injury-dependent changes in Notch ligand and receptor gene expression. **a**, Total retinal RNA was used for PCR analysis of Notch ligand and receptor gene expression at various times post injury. **b**, Percentage of indicated retinal cell types expressing the indicated gene based on data from Hoang et al., 2020. **c**, GFP and mCherry immunofluorescence on adult retinal sections from *tp1:mCherry;gfap:GFP* transgenic fish. **d**, Representative fluorescent image of mCherry immunofluorescence (red) and EdU Click-iT chemistry (green) on retinal sections at 2 and 4 dpi. Arrows point to EdU+/mCherry- MG-derived progenitors. **e**, Graph is qPCR quantification of *mCherry* RNA expression in adult retina of *tp1:mCherry* fish at various times post needle poke injury. Compared to 0 dpi, *P=0.0478 at 0.5 and 2 days post injury. **f**, Top: Experimental time line. Graph: Percentage of EdU+ cells that are also BrdU+. Right: Representative fluorescent images following DAPT treatment from 2-4 dpi in the needle pole injured retina (EdU+ cells are green and BrdU+ cells are red). Arrows point to double labelled cells. Abbreviations: ONL, outer nuclear layer; INL, inner nuclear layer; GCL, ganglion cell layer. Scale bar is 100 μm.

Figure 5-figure supplement 5: Notch ligand encoding genes that regulate MG's injury response. **a**, *dlb*-MO suppresses *dlb-GFP* chimeric RNA expression in embryos. Numbers in panels refer to number of lissamine+ fish with GFP+ phenotype. **b**, Experimental time line and EdU Click-iT chemistry on retinal sections to detect proliferating cells. **c**, Quantification of EdU+ cells in control and Dlb knockdown retinas; *P<0.0446. **d**, Quantification of the proliferative zone in the injured zebrafish retina treated with control and *dlb*-MO; ***P<0.0001. **e**, PCR analysis of *dll4* RNA expression in retinas treated with control and *dlb*-MO. **f**, Experimental time line and EdU Click-iT chemistry on retinal sections to identify proliferating cells. **g**, Quantification of EdU+ cells in control (Wt) and Dlb overexpressing (Dlb) transgenic fish; **P=0.0018. **h**, PCR shows *dll4*-MO stimulates intron retention in the *dll4* RNA. **i**, CRISPR-based

gene editing detected in genomic DNA from *ubi:Cas9;u6:dll4gRNA*$_{1,2}$ transgenic fish. **j**, qPCR analysis of *dll4* transgene induction in *hsp70:dll4-p2A-GFP* fish after heat shock. Abbreviations: MO, morpholino; C-MO or Con-MO, control-MO; n3-MO, notch3-MO; ONL, outer nuclear layer; INL, inner nuclear layer; GCL, ganglion cell layer. Scale bars are 100 μm.

Figure 5-figure supplement 6: Notch3 regulates MG's threshold response to injury. **a**, Diagram of the *notch3* gene with MO and gRNA target sites indicated. **b**, *notch3*-MO suppresses *notch3-GFP* chimeric RNA expression in embryos. Numbers in panels refer to number of lissamine+ fish with GFP+ phenotype. **c, h,** EdU Click-iT assay on retinal sections at 4 dpi to detect proliferating cells. **d, i,** Quantification of the number of EdU+ cells at 4 dpi; (**d**) Compared to C-MO, ***P*=0.0019 (0.2mM), ***P*=0.0015 (0.5mM), ****P*=0.0006 (1mM); (**i**) compared to Cas9 ****P*=0.0002. **e, j,** Quantification of the width of the proliferative zone in retinas at 4 dpi; (**e**) ****P*<0.0001; (**j**) ****P*<0.0001; **f, k,** Quantification of TUNEL+ cells at 1 dpi. **g**, CRISPR-based gene editing detected by PCR using genomic DNA from transgenic fish. Abbreviations: MO, morpholino; C-MO or Con-MO, control-MO; n3-MO, notch3-MO; ONL, outer nuclear layer; INL, inner nuclear layer; GCL, ganglion cell layer. Scale bars are 100 μm.

Figure 7-figure supplement 7: Notch signaling in developing and adult fish retina. **a**, PCR and agarose gel analysis of *mCherry* and *gapdh*$_s$ RNA expression in adult *tp1:mCherry* fish treated +/-DAPT. **b**, Top: PCR and agarose gel analysis of *mCherry* RNA expression in developing *tp1:mCherry* fish. Bottom graph: qPCR analysis of *mCherry* RNA expression in retinas of developing *tp1:mCherry* fish. Compared to 2 dpf, **P*=0.0252 (5dpf), ***P*=0.0076 (7dpf), **P*=0.0122 (15dpf), ***P*=0.0065 (1mpf), ***P*=0.0074 (2mpf), ***P*=0.0016 (4mpf), ****P*=0.0008 (6mpf). Abbreviations: d, days; m, months. Scale bar is 100 μm.

Supplementary Tables

Table S1: Inj reg genes & chromatin. Related to Figure 1.

Table S2: Inj reg ATAC genes, promoters, & 1-5kb regions. Related to Figure 1.

Table S3: Inj and DAPT coordinately regulated genes. Related to Figure 2.

Table S4: DAPT & inj regulated ATACseq. Related to Figure 2.

Table S5: DAPT & DN-MAML intersection with regeneration-associated genes. Related to Figure 2.

Table S6: PCR heat map data. Related to Figure 4.

Table S7: Primer, MO, gRNA list. Related to Material and methods.

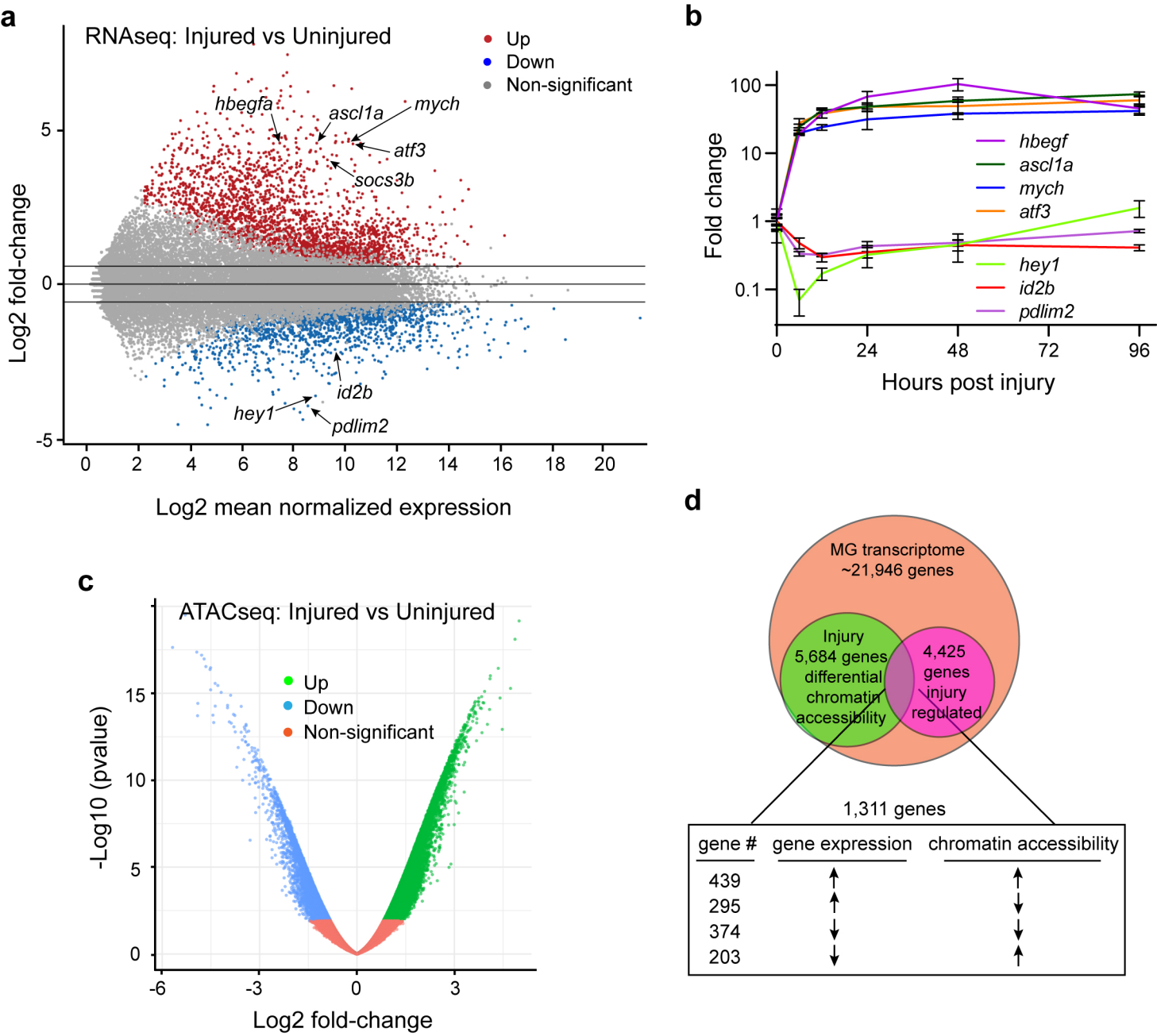
a
RNAseq: Injured vs Uninjured
Up
Down
Non-significant
hbegfa
ascl1a
mych
atf3
socs3b
id2b
hey1
pdlim2
Log2 fold-change
Log2 mean normalized expression
b
Fold change
Hours post injury
hbegf
ascl1a
mych
atf3
hey1
id2b
pdlim2
c
ATACseq: Injured vs Uninjured
Up
Down
Non-significant
-Log10 (pvalue)
Log2 fold-change
d
MG transcriptome
~21,946 genes
Injury
5,684 genes
differential
chromatin
accessibility
4,425
genes
injury
regulated
1,311 genes
gene #
gene expression
chromatin accessibility
439
295
374
203

Fig. 1

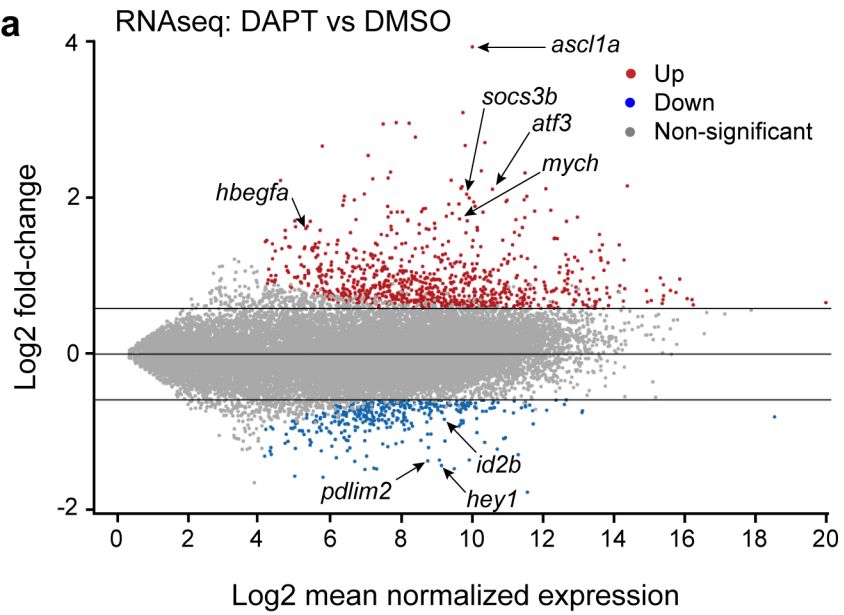
a
RNAseq: DAPT vs DMSO
ascl1a
socs3b
atf3
mych
hbegfa
id2b
pdlim2
hey1
Up
Down
Non-significant
Log2 fold-change
Log2 mean normalized expression

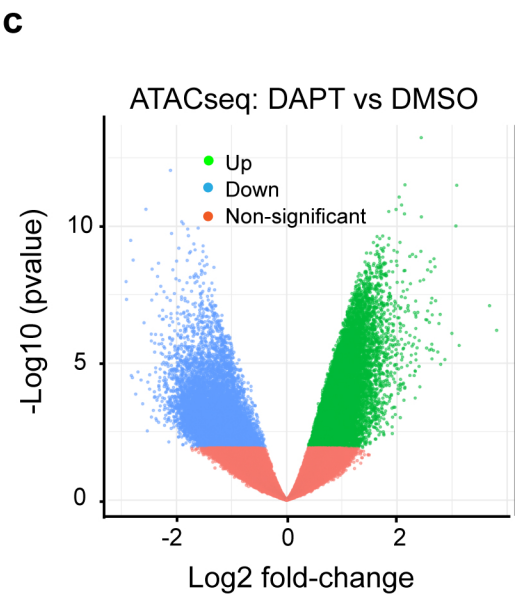
c
ATACseq: DAPT vs DMSO
Up
Down
Non-significant
-Log10 (pvalue)
Log2 fold-change

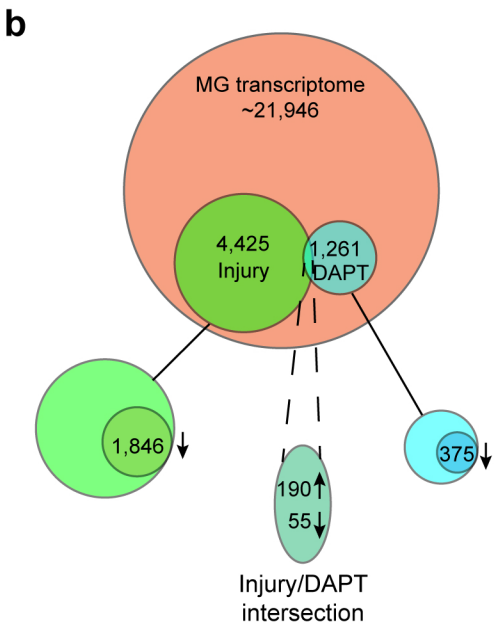
b
MG transcriptome
~21,946
4,425
Injury
1,261
DAPT
1,846
190
55
375
Injury/DAPT
intersection

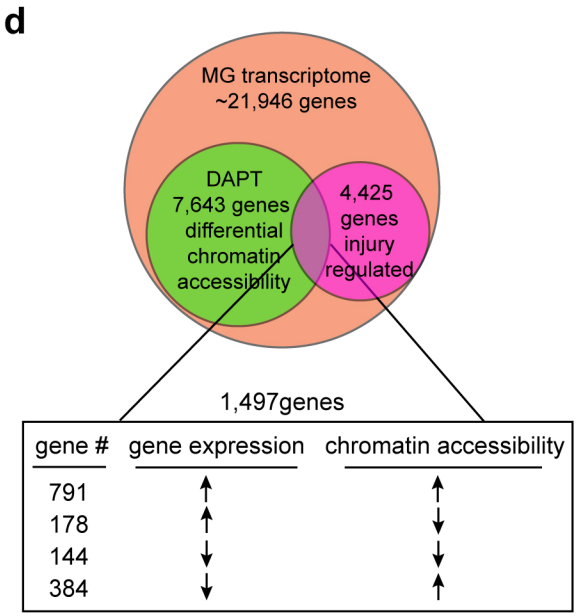
d
MG transcriptome
~21,946 genes
DAPT
7,643 genes
differential
chromatin
accessibility
4,425
genes
injury
regulated
1,497genes
gene #
gene expression
chromatin accessibility
791
178
144
384

Fig. 2

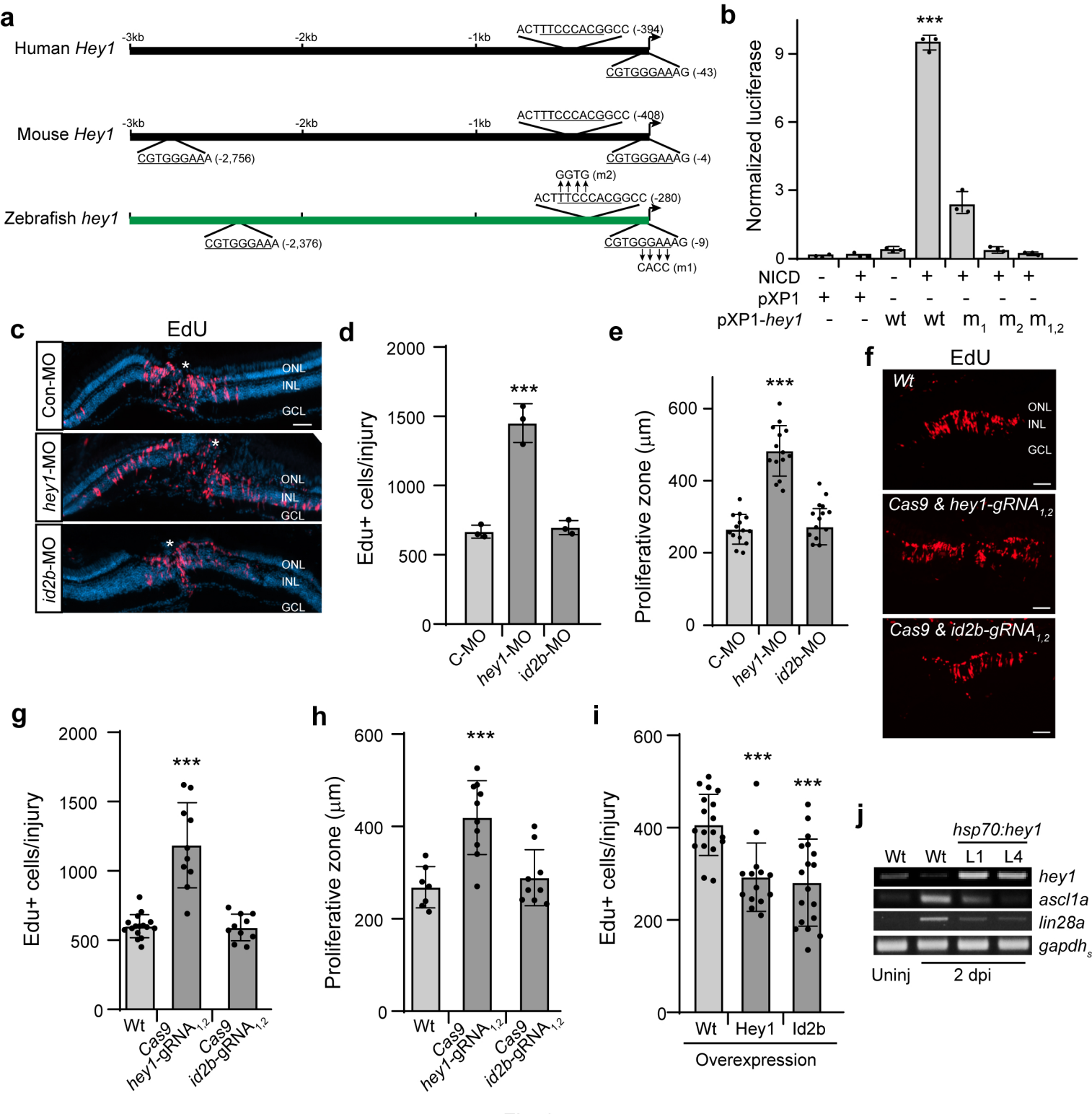
a
Human Hey1
-3kb
-2kb
-1kb
ACTTTCCCACGGCC (-394)
CGTGGGAAAG (-43)
Mouse Hey1
ACTTTCCCACGGCC (-408)
CGTGGGAAA (-2,756)
CGTGGGAAAG (-4)
Zebrafish hey1
GGTG (m2)
ACTTTCCCACGGCC (-280)
CGTGGGAAA (-2,376)
CGTGGGAAAG (-9)
CACC (m1)
b
Normalized luciferase
***
NICD
pXP1
pXP1-hey1
wt
m1
m2
m1,2
c
EdU
Con-MO
hey1-MO
id2b-MO
ONL
INL
GCL
d
Edu+ cells/injury
C-MO
e
Proliferative zone (µm)
f
Wt
Cas9 & hey1-gRNA1,2
Cas9 & id2b-gRNA1,2
g
Wt
Cas9 hey1-gRNA1,2
Cas9 id2b-gRNA1,2
h
i
Hey1
Id2b
Overexpression
j
hsp70:hey1
L1
L4
hey1
ascl1a
lin28a
gapdhs
Uninj
2 dpi

Fig. 3

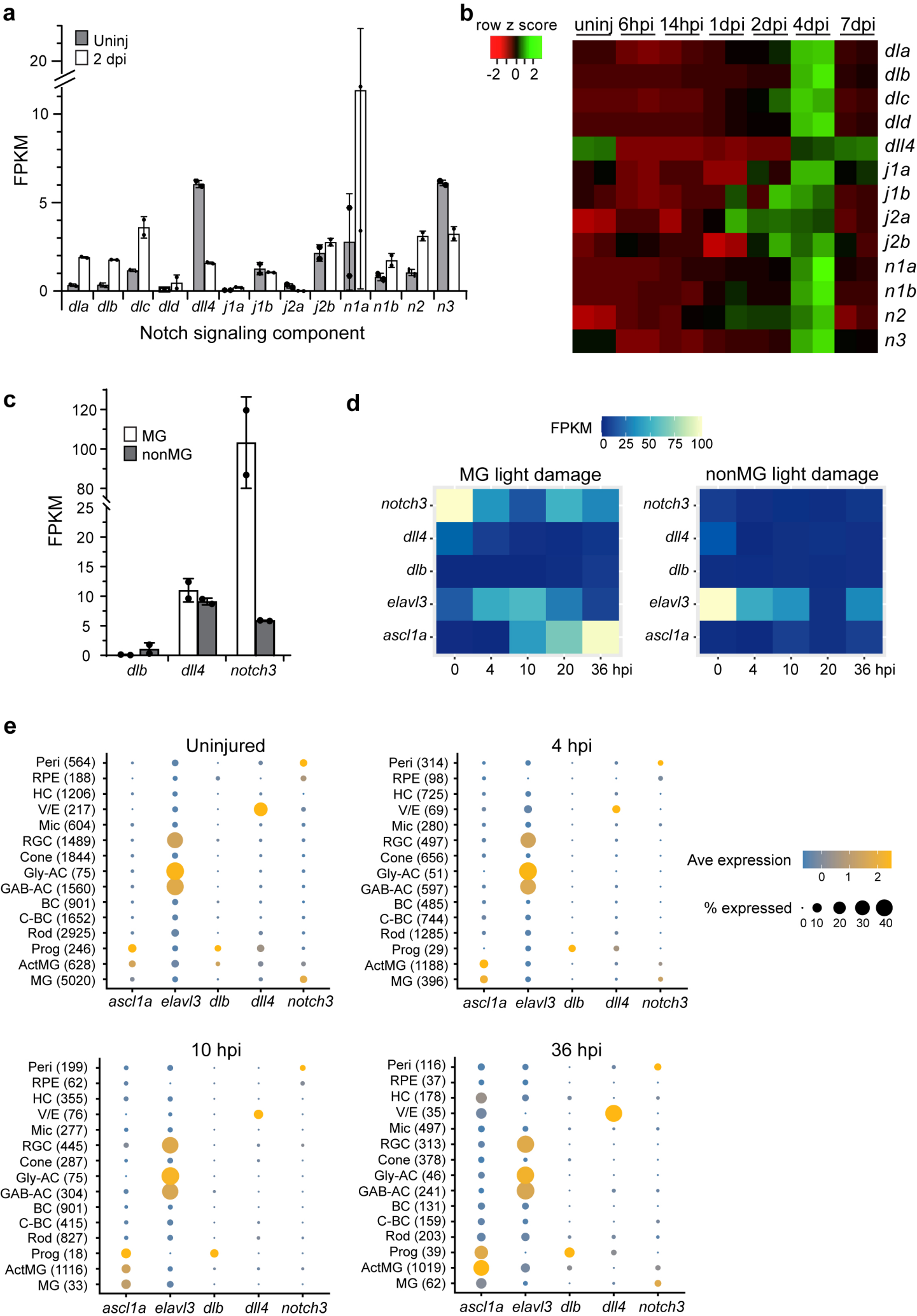
a
Uninj
2 dpi
FPKM
dla dlb dlc dld dll4 j1a j1b j2a j2b n1a n1b n2 n3
Notch signaling component
b
row z score
-2 0 2
uninj 6hpi 14hpi 1dpi 2dpi 4dpi 7dpi
dla dlb dlc dld dll4 j1a j1b j2a j2b n1a n1b n2 n3
c
MG
nonMG
FPKM
dlb dll4 notch3
d
FPKM
0 25 50 75 100
MG light damage
nonMG light damage
notch3 dll4 dlb elavl3 ascl1a
0 4 10 20 36 hpi
e
Uninjured
4 hpi
10 hpi
36 hpi
Peri RPE HC V/E Mic RGC Cone Gly-AC GAB-AC BC C-BC Rod Prog ActMG MG
ascl1a elavl3 dlb dll4 notch3
Ave expression
0 1 2
% expressed
0 10 20 30 40

Fig. 4

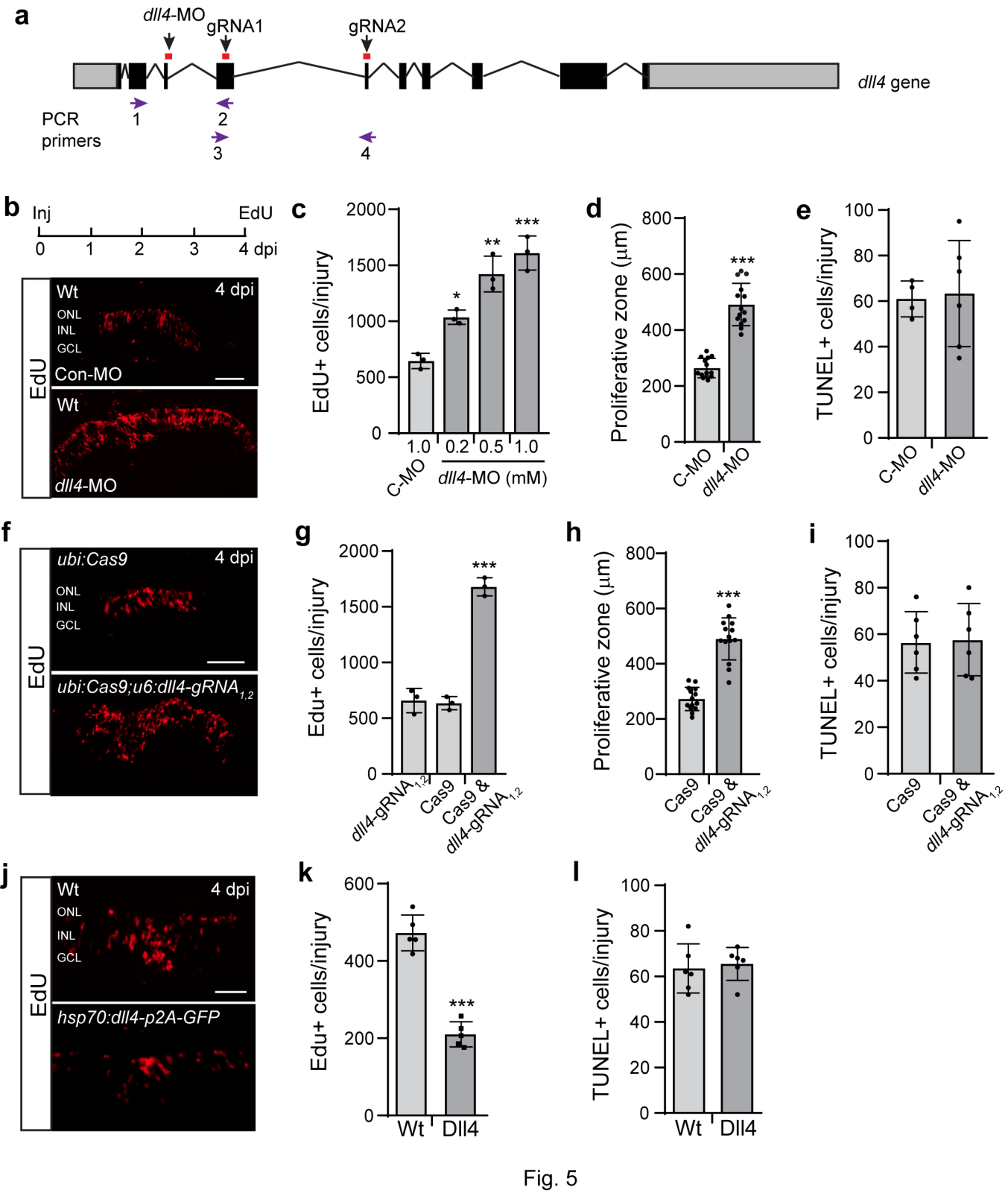
a
dll4-MO
gRNA1
gRNA2
dll4 gene
PCR primers
1
2
3
4
b
Inj
EdU
0 1 2 3 4 dpi
Wt
4 dpi
ONL
INL
GCL
Con-MO
Wt
dll4-MO
EdU
c
EdU+ cells/injury
1.0
0.2
0.5
1.0
C-MO
dll4-MO (mM)
d
Proliferative zone (µm)
C-MO
dll4-MO
e
TUNEL+ cells/injury
C-MO
dll4-MO
f
ubi:Cas9
4 dpi
ONL
INL
GCL
ubi:Cas9;u6:dll4-gRNA1,2
EdU
g
Edu+ cells/injury
dll4-gRNA1,2
Cas9
Cas9 & dll4-gRNA1,2
h
Proliferative zone (µm)
Cas9
Cas9 & dll4-gRNA1,2
i
TUNEL+ cells/injury
Cas9
Cas9 & dll4-gRNA1,2
j
Wt
4 dpi
ONL
INL
GCL
hsp70:dll4-p2A-GFP
EdU
k
Edu+ cells/injury
Wt
Dll4
l
TUNEL+ cells/injury
Wt
Dll4

Fig. 5

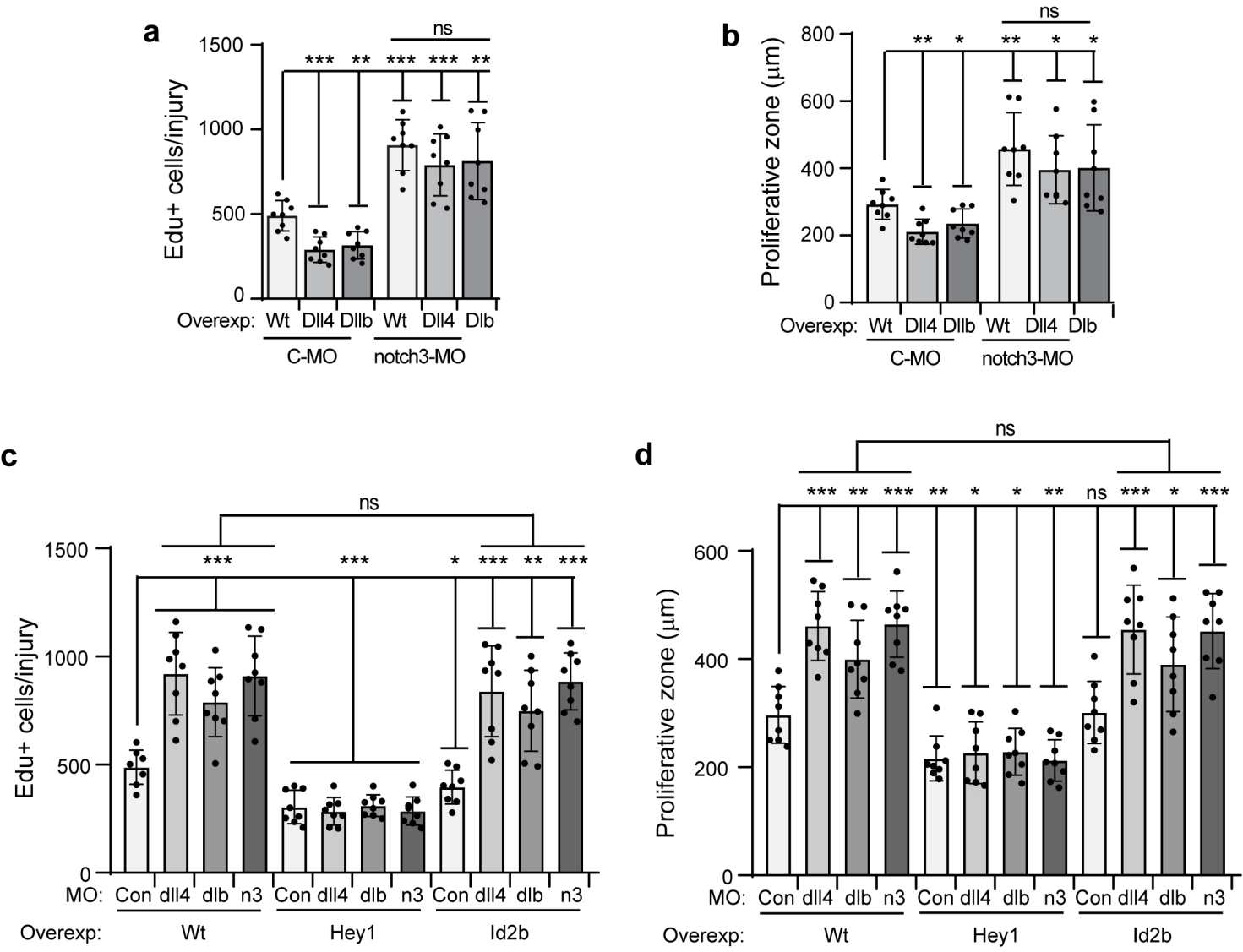
a
Edu+ cells/injury
1500
1000
500
0
ns
***
**
***
***
**
Overexp: Wt Dll4 Dllb Wt Dll4 Dlb
C-MO
notch3-MO
b
Proliferative zone (μm)
800
600
400
200
0
ns
**
*
**
*
*
Overexp: Wt Dll4 Dllb Wt Dll4 Dlb
C-MO
notch3-MO
c
Edu+ cells/injury
1500
1000
500
0
ns
***
***
*
***
**
***
MO: Con dll4 dlb n3 Con dll4 dlb n3 Con dll4 dlb n3
Overexp: Wt Hey1 Id2b
d
Proliferative zone (μm)
600
400
200
0
ns
***
**
***
**
*
*
**
ns
***
*
***
MO: Con dll4 dlb n3 Con dll4 dlb n3 Con dll4 dlb n3
Overexp: Wt Hey1 Id2b

Fig. 6

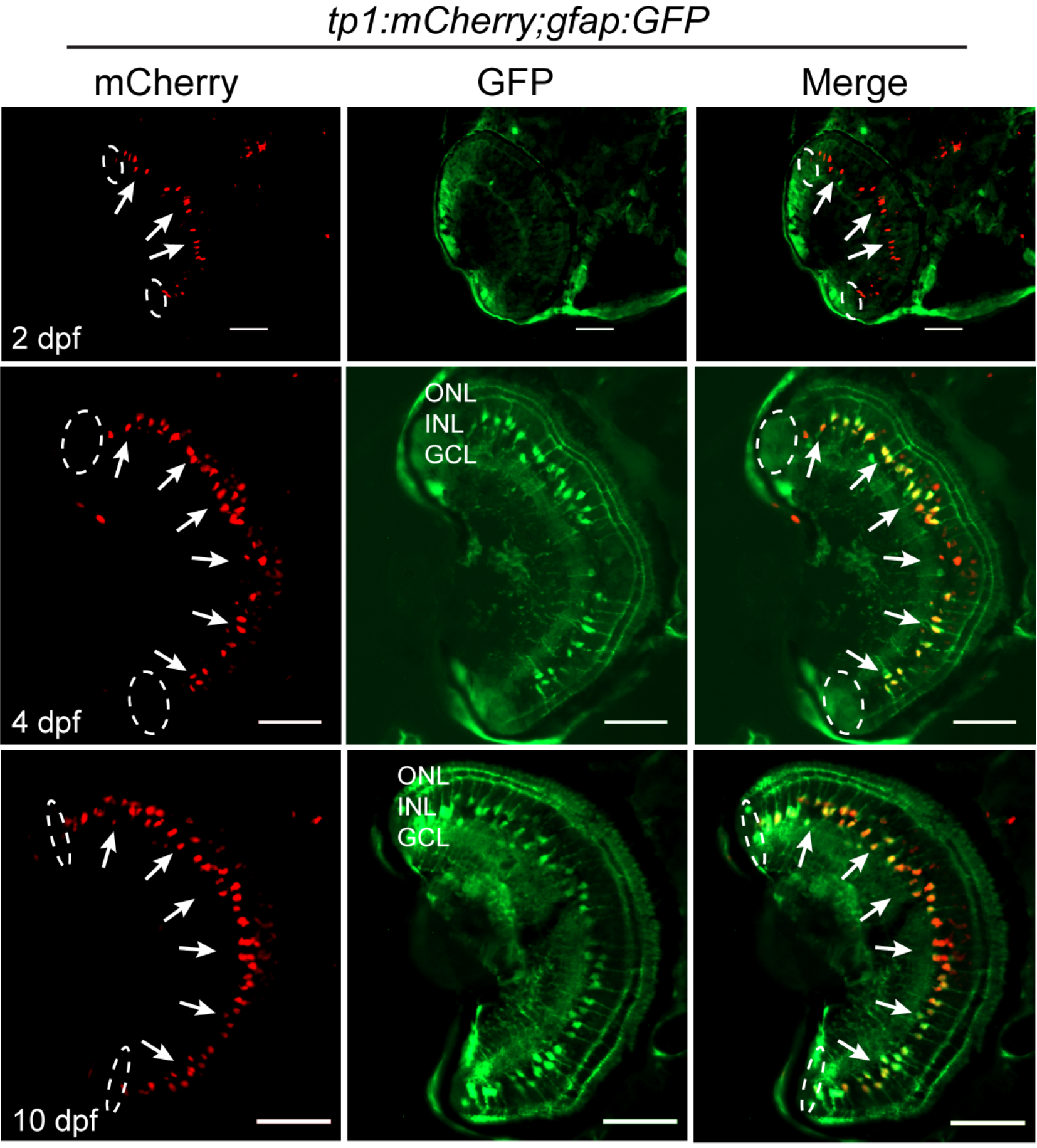
tp1:mCherry;gfap:GFP
mCherry
GFP
Merge
2 dpf
4 dpf
10 dpf
ONL
INL
GCL
ONL
INL
GCL

Fig. 7

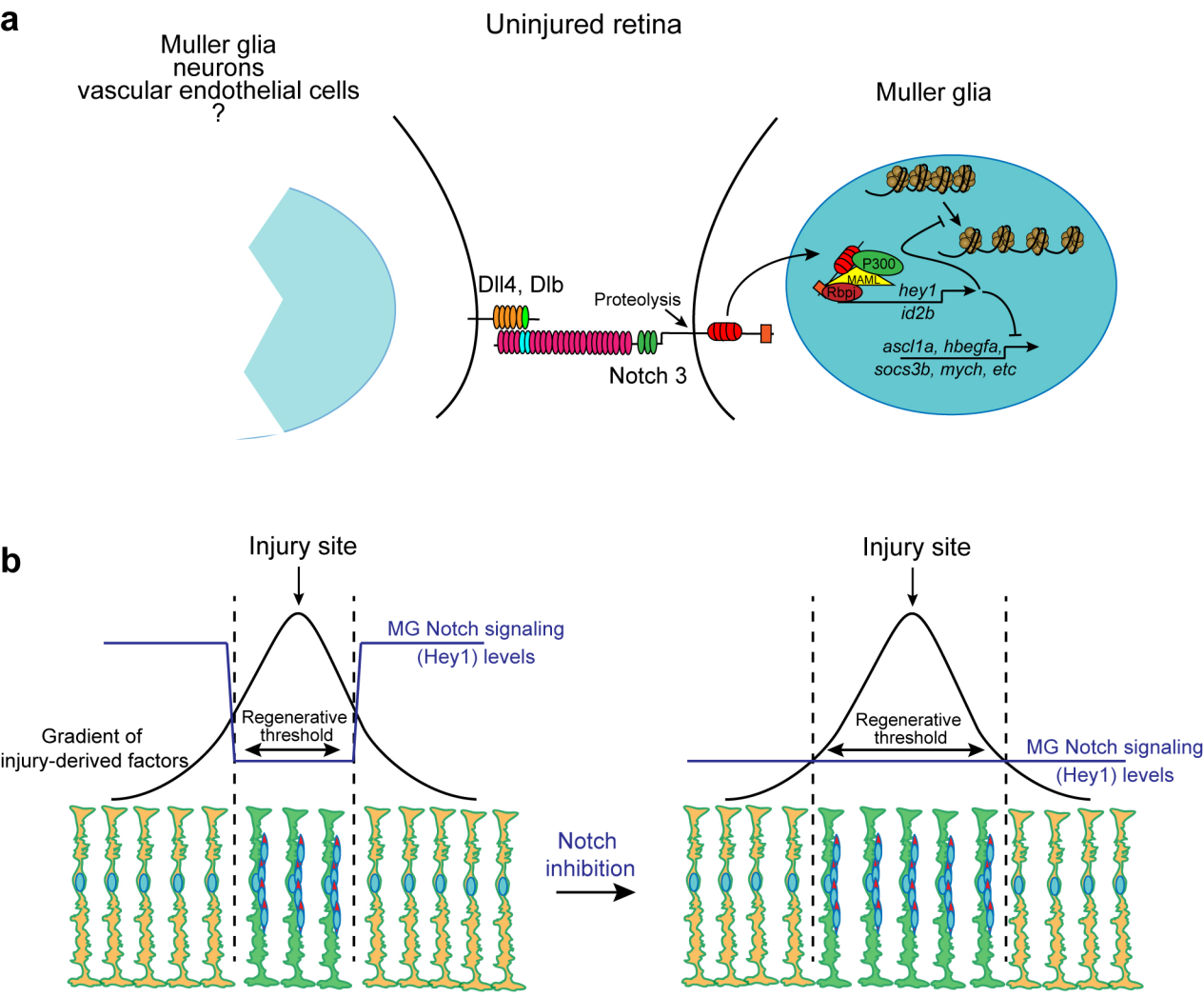
a
Uninjured retina
Muller glia
neurons
vascular endothelial cells
?
Muller glia
Dll4, Dlb
Proteolysis
Notch 3
P300
MAML
Rbpj
hey1
id2b
ascl1a, hbegfa,
socs3b, mych, etc
b
Injury site
MG Notch signaling
(Hey1) levels
Regenerative
threshold
Gradient of
injury-derived factors
Notch
inhibition
Injury site
Regenerative
threshold
MG Notch signaling
(Hey1) levels

Fig. 8

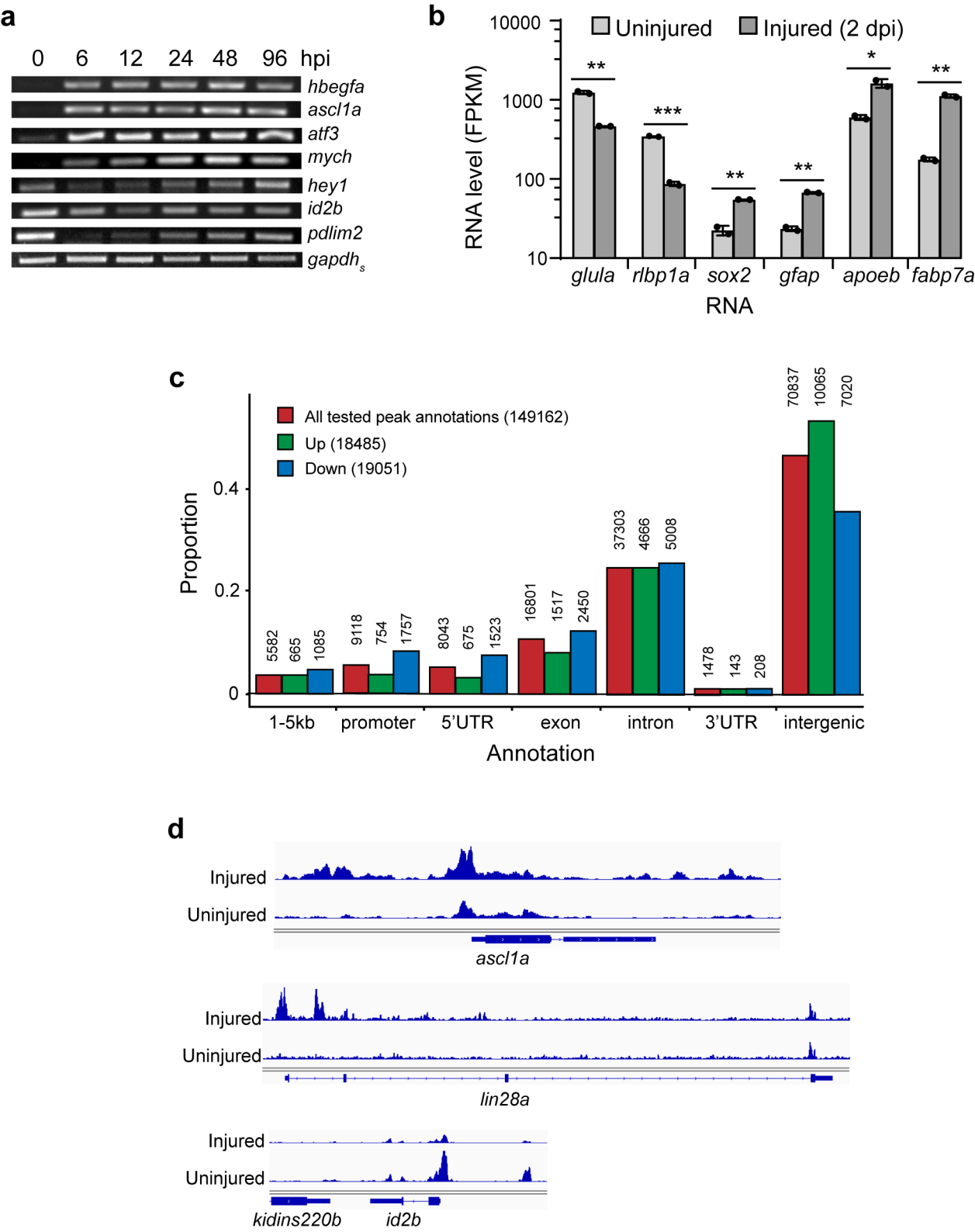

Supplementary Fig. S1

a

Top 20 injury-responsive genes

Inj/DAPT-induced	Inj/DAPT-suppressed
*fabp11a**	*pdlim2*
flnca	*hey1**
*kng1**	*vcam1*
cpa2	*cryba4**
*fosl1a**	*scn4aa*
nrd1a	*metrn*
*mych**	*id2b**
*f3a**	*gpsm1b*
*hbegfa**	*kera*
*ascl1a**	*arhgef28*
atf3	*npas3b*
slc2a6	*rasfgrf2b*
tubb6	*kcnv1*
cebpb	*rhobtb2b*
*socs3b**	*fabp1a*
ctgfa	*cdh16*
knstrn	*actr3b*
cxcl18b	*her12*
mcoln2	*soga*
jun	*klfl18*

b

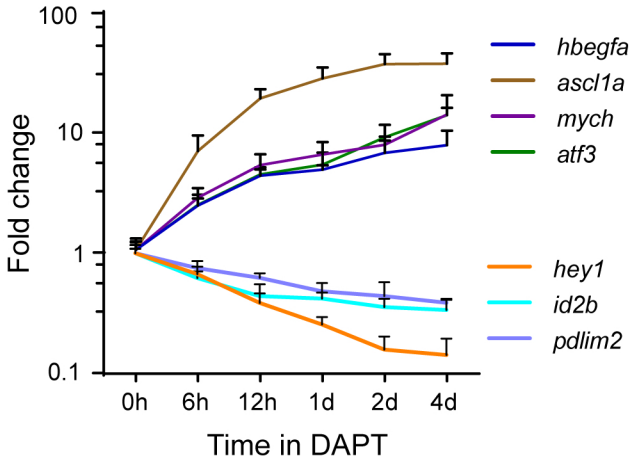

c

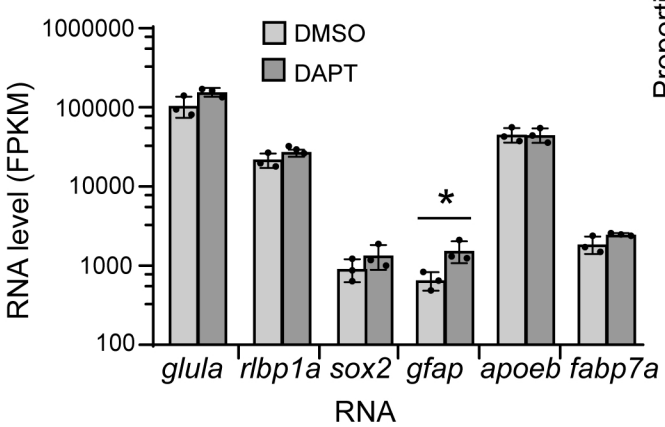

d

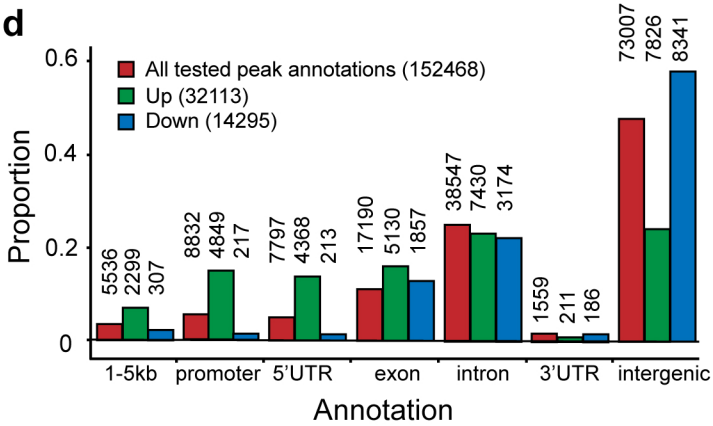

e

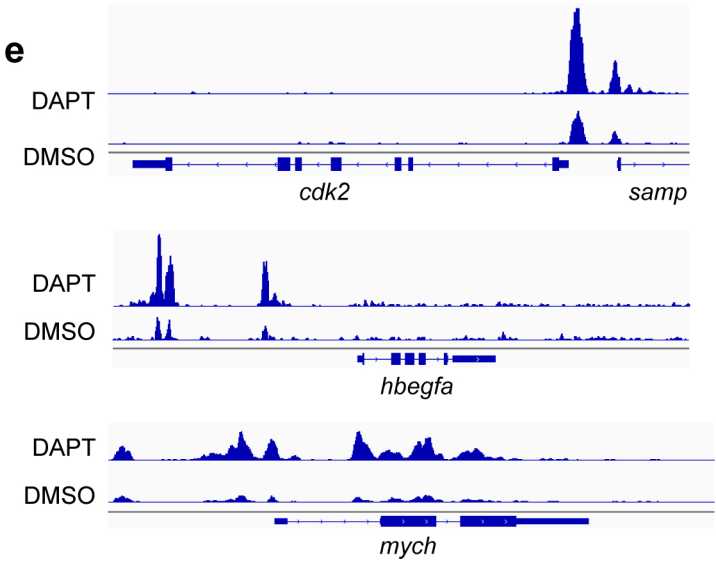

f

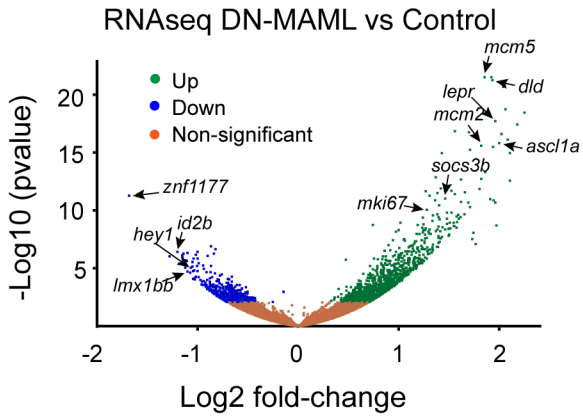

Supplementary Fig. S2

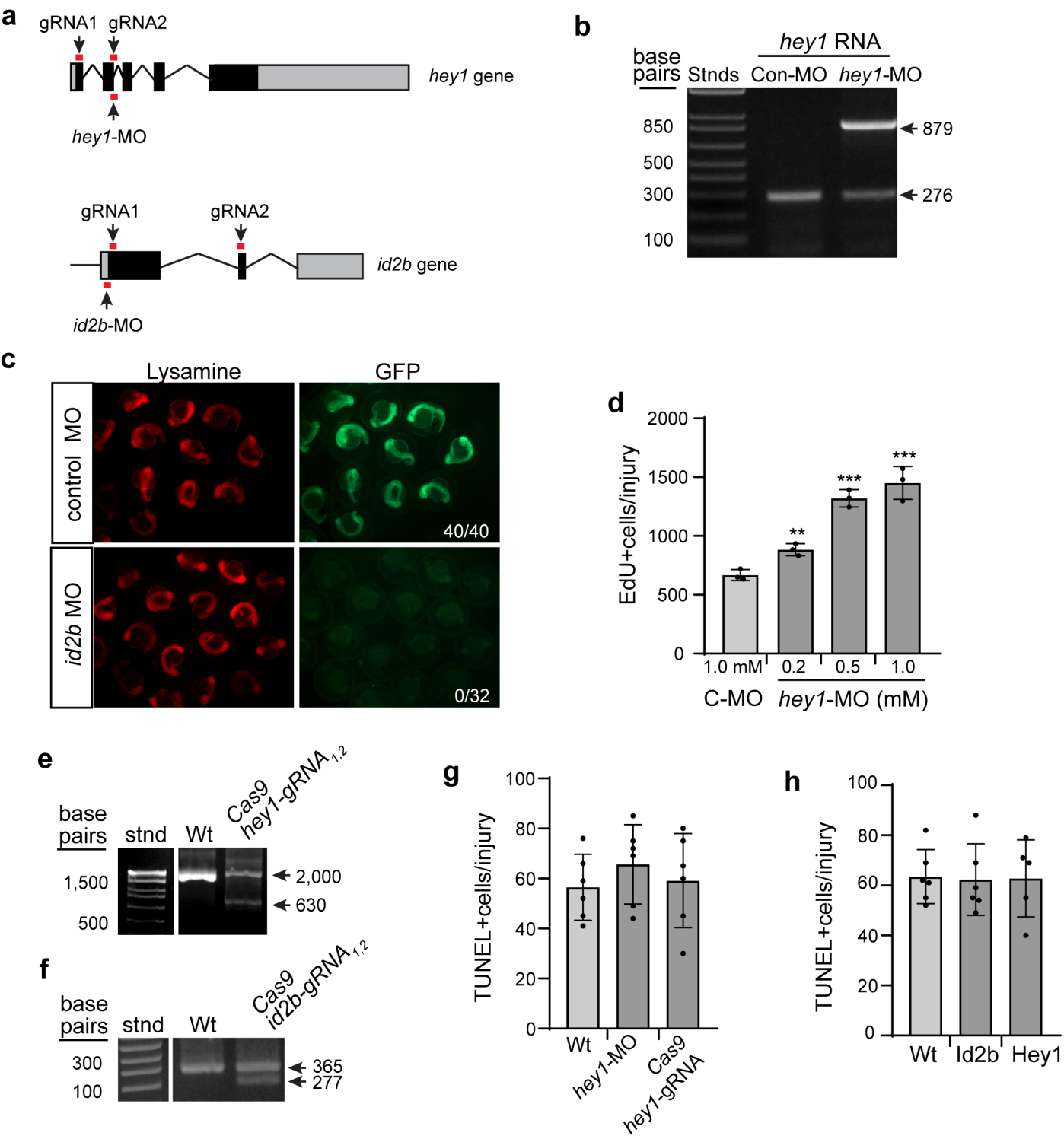

Supplementary Fig. S3

a

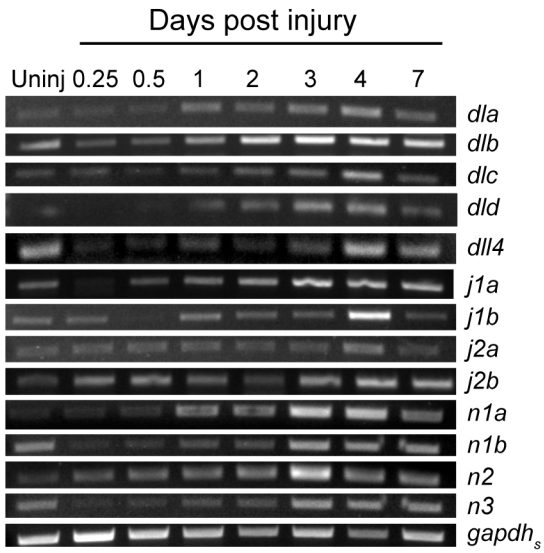

b

Cell type	*dlb (%)*	*dll4 (%)*	*notch3 (%)*	Total cells
Resting MG	4 (0.05)	53 (0.68)	334 (4.3)	7738
Activated MG	116 (1.7)	34 (0.49)	104 (1.51)	6905
Neurons	40 (0.16)	91 (0.36)	61 (1.51)	25395
Microglia	5 (0.20)	2 (0.08)	5 (0.20)	2520
V/E	0 (0)	95 (22)	2 (0.47)	427
Progenitors	19 (4.3)	16 (3.59)	1 (0.22)	446

scRNAseq data from Hoang et al., 2020 was interrogated for gene expression data. Values are the number of cells exhibiting expression above background in the uninjured retina.

c

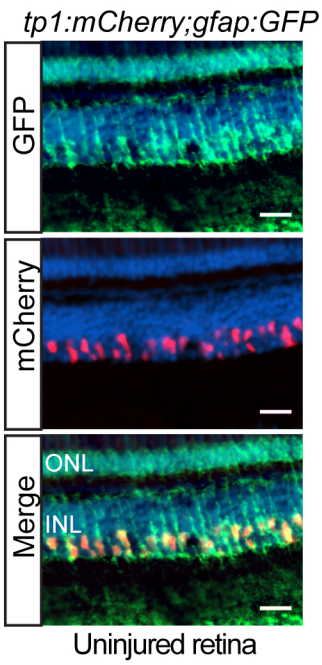

d

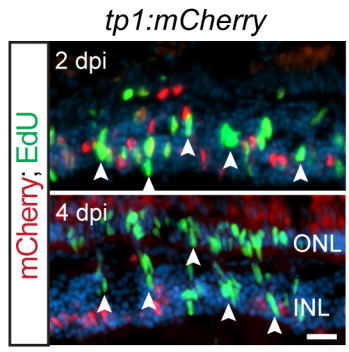

e

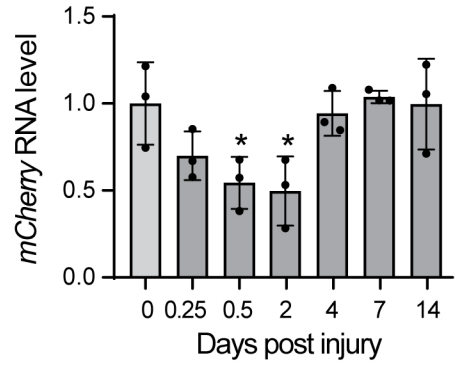

f

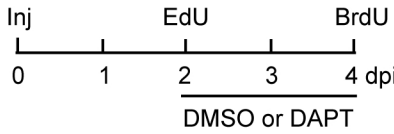

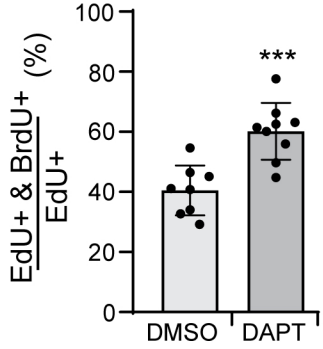

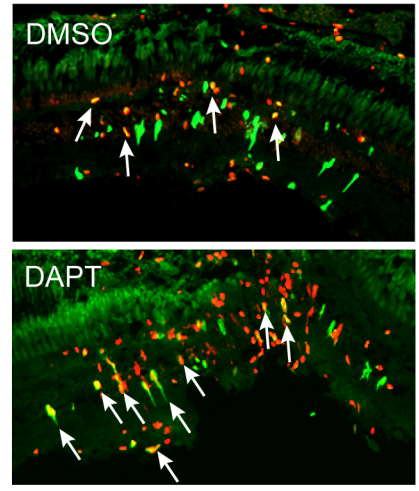

Supplementary Fig. S4

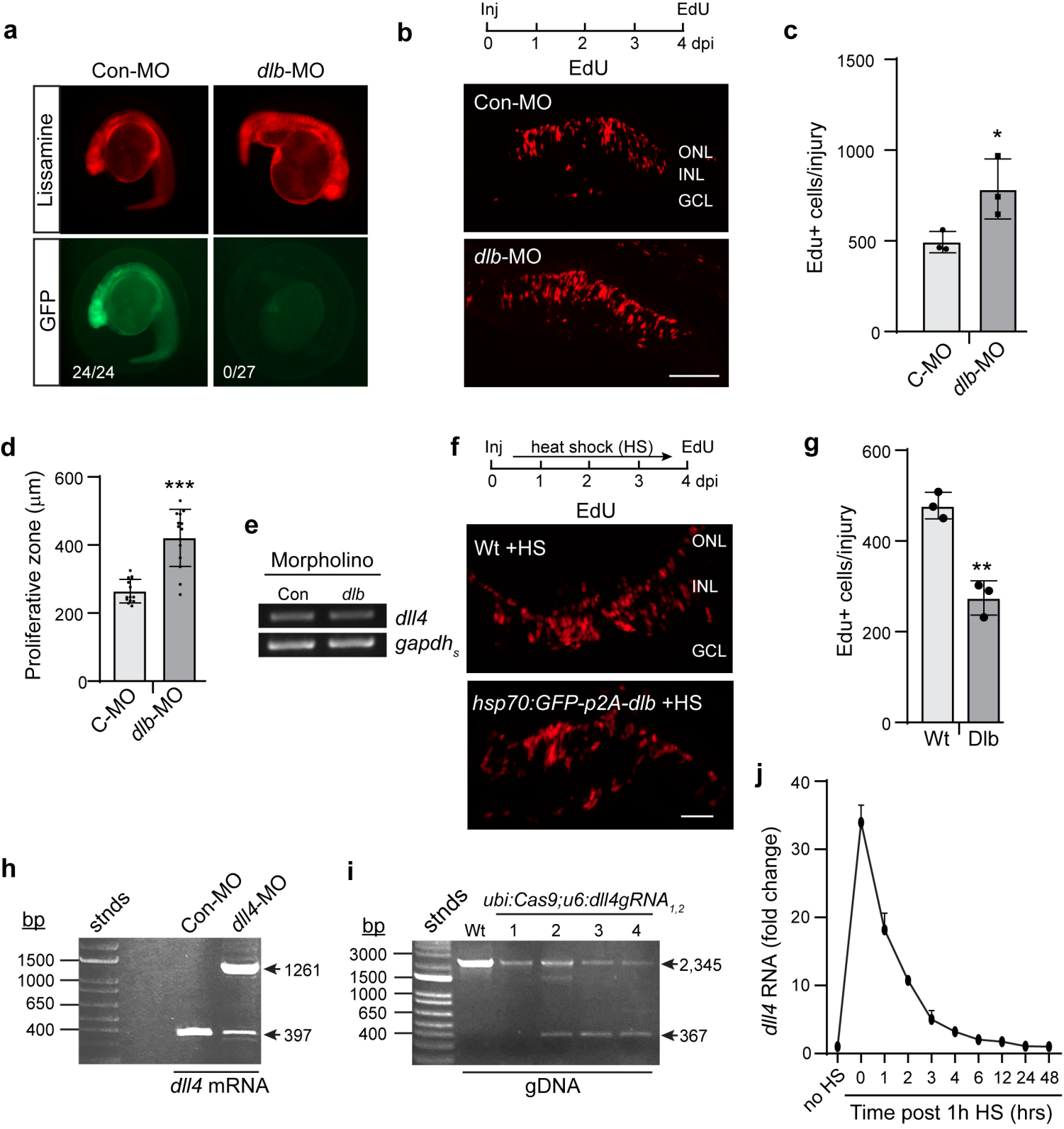

Supplementary Fig. S5

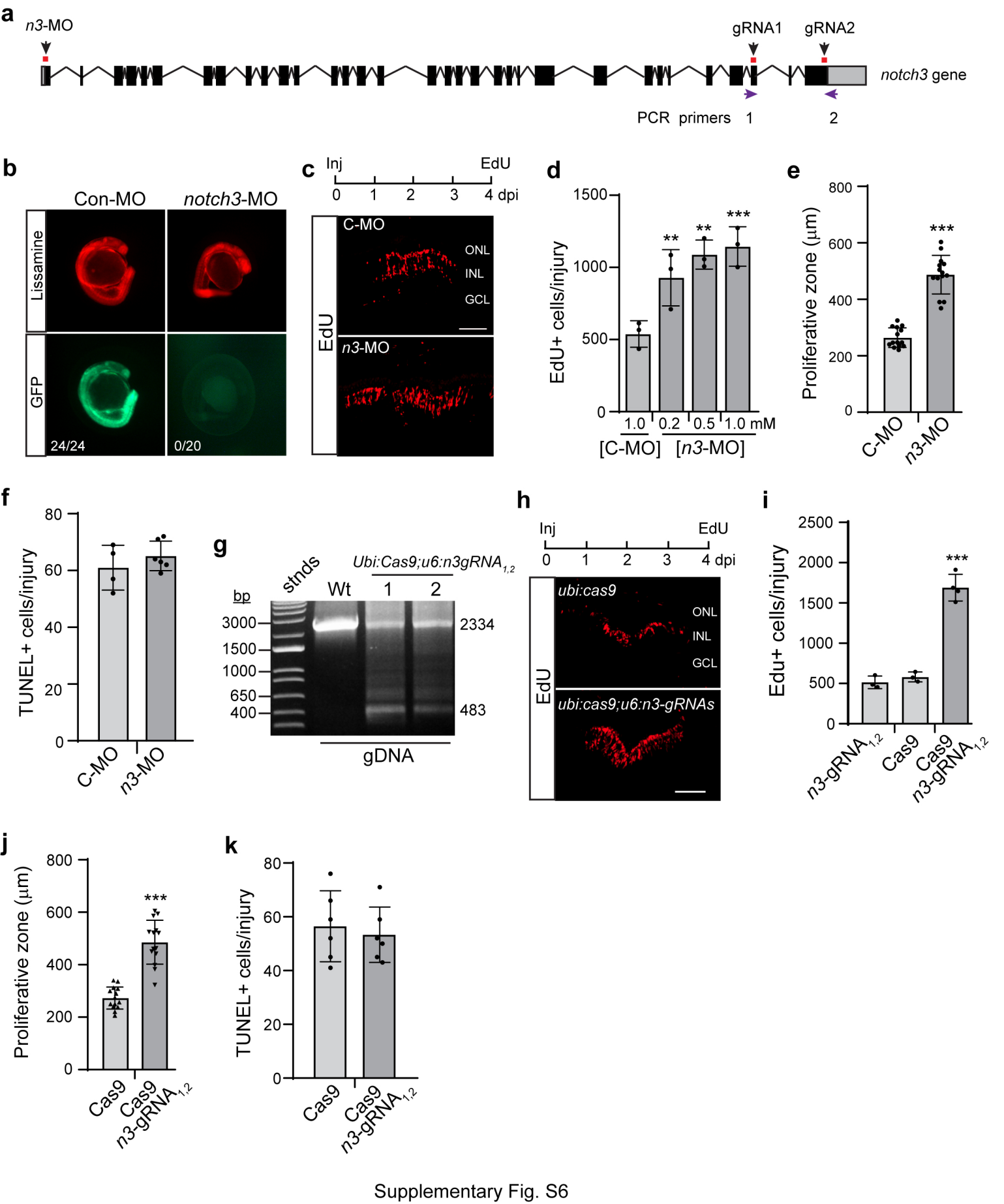

Supplementary Fig. S6

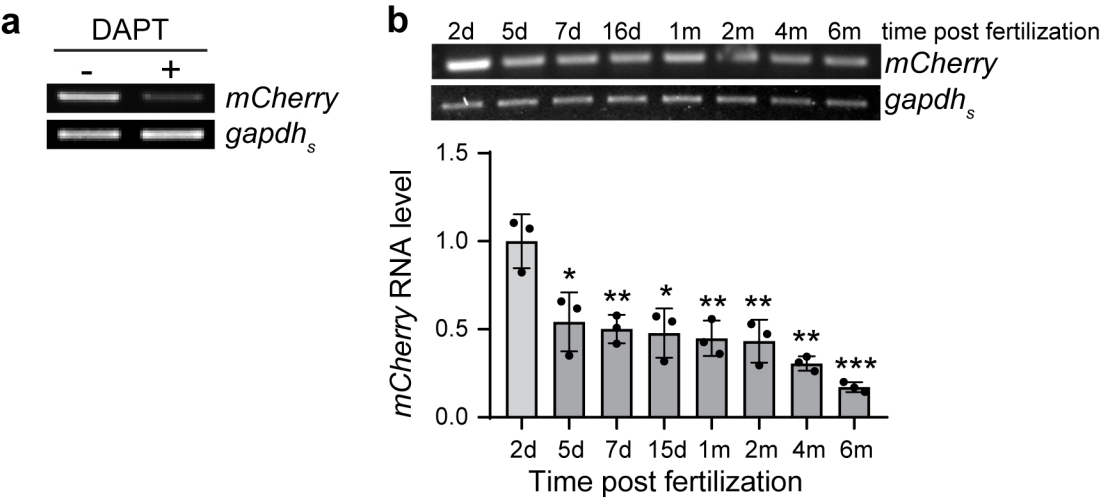

Supplementary Fig. S7